ARTICLE

Subsets of cancer cells expressing CX3CR1 are endowed with metastasis-initiating properties and resistance to chemotherapy

Anthony DiNatale[1], Ramanpreet Kaur[1,6,9], Chen Qian[1,7,9], Jieyi Zhang[1], Michael Marchioli[1], Darin Ipe[1], Maria Castelli[1,8], Chris M. McNair[2,3], Gaurav Kumar[2], Olimpia Meucci[1,4] and Alessandro Fatatis[1,5]✉

Metastasis-initiating cells (MICs) display stem cell-like features, cause metastatic recurrences and defy chemotherapy, which leads to patients' demise. Here we show that prostate and breast cancer patients harbor contingents of tumor cells with high expression of CX3CR1, OCT4a (POU5F1), and NANOG. Impairing CX3CR1 expression or signaling hampered the formation of tumor spheroids by cell lines from which we isolated small subsets co-expressing CX3CR1 and stemness-related markers, similarly to patients' tumors. These rare CX3CR1^{High} cells show transcriptomic profiles enriched in pathways that regulate pluripotency and endowed with metastasis-initiating behavior in murine models. Cancer cells lacking these features (CX3CR1^{Low}) were capable of re-acquiring CX3CR1-associated features over time, implying that MICs can continuously emerge from non-stem cancer cells. CX3CR1 expression also conferred resistance to docetaxel, and prolonged treatment with docetaxel selected CX3CR1^{High} phenotypes with de-enriched transcriptomic profiles for apoptotic pathways. These findings nominate CX3CR1 as a novel marker of stem-like tumor cells and provide conceptual ground for future development of approaches targeting CX3CR1 signaling and (re)expression as therapeutic means to prevent or contain metastasis initiation.

Oncogene; https://doi.org/10.1038/s41388-021-02174-w

INTRODUCTION

Deaths from cancer over the last decade have declined, due to progress in early detection and treatment [1]. However, a diagnosis of stage-IV disease, in which cancer cells have spread to and colonized organs away from the primary tumor, still inexorably infers a lack of curative options. Metastases can often be effectively treated, but rarely—if ever–eradicated. Thus, for most solid tumors, patients succumb to metastatic disease [2–4].

Tumors spread to distant organs by shedding circulating tumor cells (CTCs) in the blood [5]. CTCs may egress the systemic circulation, infiltrate surrounding target tissues and convert into disseminated tumor cells (DTCs), which are the seeds of metastatic lesions [6, 7]. However, most cancer cells lack the ability to initiate new tumors, and this peculiarity also extends to DTCs in target organs [8]. Thus, both early metastases and the subsequent secondary tumors generated by metastasis-to-metastasis expansion [9–11] depend on the unique properties of a minority of cancer cells endowed with the ability to both colonize a tissue and sustain long-term tumor growth [12]. These metastasis-initiating cells (MICs) must adapt to new organ microenvironments, benefiting from trophic factors normally present in the target tissue or produced by resident stromal cells in response to tumor-derived signals [13, 14]. DTCs arrive at and initially inhabit tissues as either isolated units or small clusters that often lack interclonal cooperation, a key promoter of tumor growth [15]. This is a major attrition point in the metastatic process, as MICs must recruit tumor-intrinsic and/or tissue-induced embryonic transcription factors that promote initial survival and subsequent proliferative expansion.

Transcription factors such as OCT4a and NANOG operate as a network of master controllers of cellular fate by inducing de-differentiation and tightly regulating their own expression and that of multiple other genes involved in pluripotency pathways [16, 17]. These embryonic factors are re-expressed in poorly differentiated, aggressive tumors [18], and the pathways they control are reactivated in rare cancer cells that can start primary tumors, including cancer stem cells (CSCs) or tumor-initiating cells (TICs). TICs are considered functionally similar—albeit not identical–to MICs, which additionally need to survive in circulation and adapt to organ microenvironments that are significantly different from the primary tumor of origin [12, 19].

A major stemness feature is self-renewal, by which a CSC divides asymmetrically into a new CSC—to preserve the pool—and a differentiated, non-CSC [19]. However, the previously long-held unidirectional model of stem cell hierarchy might need to be reconsidered, since the evidence is emerging that non-CSCs can shift to a CSC state [20, 21]. Understandably, this phenotypic plasticity presents crucial implications for tumor growth dynamics and therapy [22, 23].

[1]Department of Pharmacology and Physiology, Drexel University College of Medicine, Philadelphia, PA 19102, USA. [2]Department of Cancer Biology, Sidney Kimmel Cancer Center of Thomas Jefferson University, Philadelphia, PA 19107, USA. [3]Cancer Informatics, Sidney Kimmel Cancer Center of Thomas Jefferson University, Philadelphia, PA 19107, USA. [4]Program in Immune Cell Regulation & Targeting, Sidney Kimmel Cancer Center of Thomas Jefferson University, Philadelphia, PA 19107, USA. [5]Program in Translational and Cellular Oncology at Sidney Kimmel Cancer Center of Thomas Jefferson University, Philadelphia, PA 19107, USA. [6]Present address: Champions Oncology, 1330 Piccard Drive, Rockville, MD 20850, USA. [7]Present address: Samuel Oschin Cancer Center, Cedars-Sinai, Los Angeles, CA 90048, USA. [8]Present address: Perelman School of Medicine, University of Pennsylvania, Philadelphia, PA 19104, USA. [9]These authors contributed equally: Ramanpreet Kaur and Chen Qian. ✉email: af39@drexel.edu

Received: 23 August 2021 Revised: 2 December 2021 Accepted: 30 December 2021
Published online: 08 January 2022

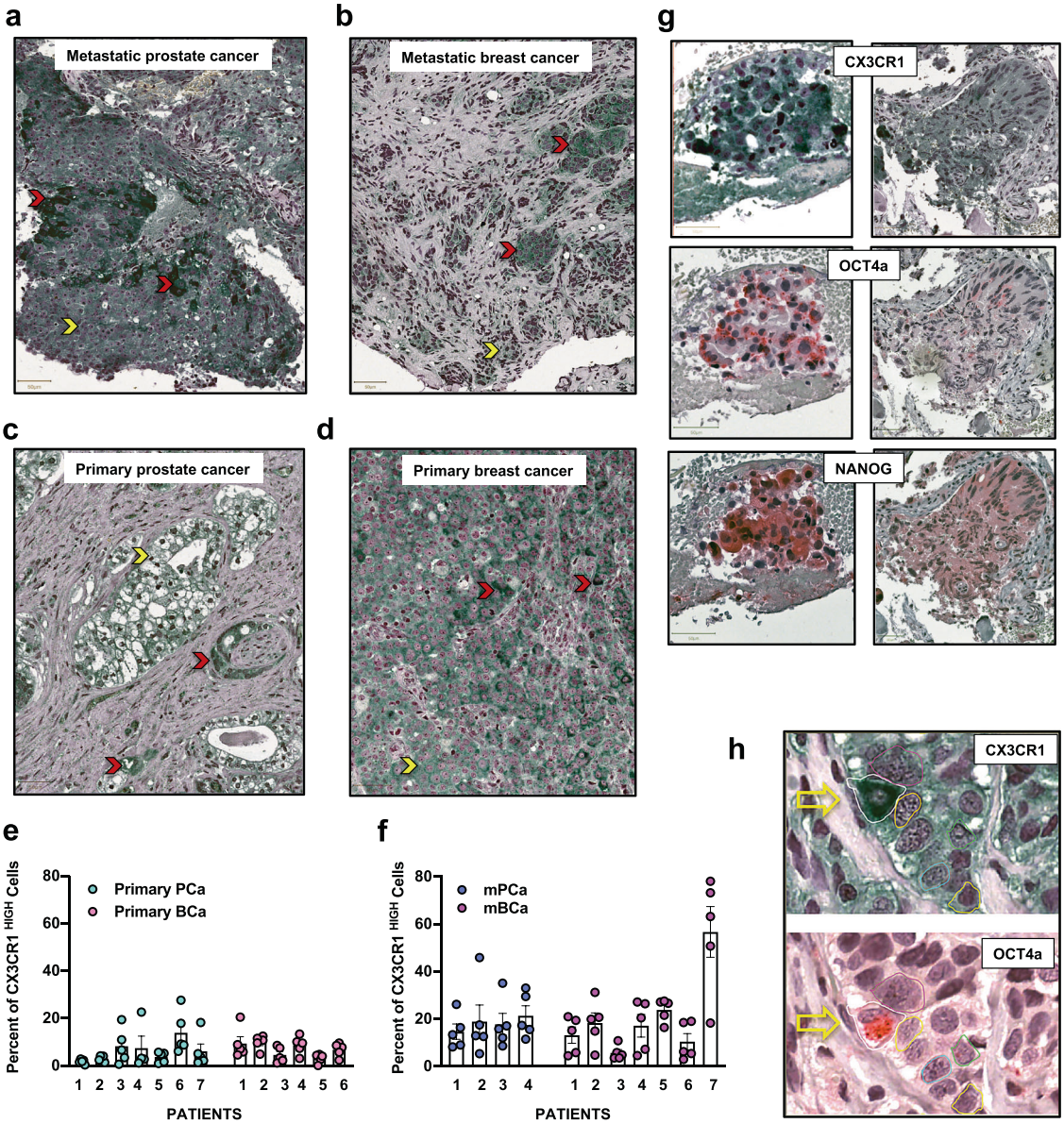

Fig. 1 CX3CR1^{High} cancer cells are detected in patient samples from primary and metastatic breast and prostate cancers. **a, b** Representative images of metastatic tumors with cancer cells showing intense CX3CR1 staining (red arrows), visualized using a StayGreen chromogen, among a majority of cells showing little or no staining for the chemokine receptor (yellow arrows). A similar scenario was observed in tissue samples from patients with primary prostate (**c**) and breast (**d**) cancers, as shown by representative images. **e, f** Quantification of CX3CR1^{High} cancer cells was conducted by acquiring ten random fields (100,000 μm^2/each) from digital micrographs for each patient sample and enumerating all cells with staining above a set threshold (see methods) using Image-J. **g** Representative images showing that CX3CR1^{High} cancer cells co-expressed OCT4a and Nanog, which were both detected using a Vector Red chromogen by staining two consecutive tissue sections immediately following each section used for CX3CR1 staining. **h** Representative images at higher magnification demonstrating co-expression of CX3CR1 and Oct4a in the same breast cancer cell. Scale bar equals 50 μm.

MICs are identified by their stem cell-like traits, such as in vitro formation of oncospheres on low-adherence substrates, slow proliferation [19, 24], and the expression of specific cell-surface markers [25, 26].

Stem cell-like features in tumors have also been associated with the expression of chemokine receptors such as CXCR4, CXCR1, and CCR5 [27], suggesting their involvement in events additional to cancer cell migration and inflammation.

CX3CR1 is a unique member of the chemokine receptor class, as it binds to only one ligand, the chemokine CX3CL1 (a.k.a Fractalkine). While one of its major physiological roles is to regulate the trafficking of immune cells to sites of inflammation, CX3CR1 is also expressed by a variety of normal and malignant cells. We and others have reported that CX3CR1 helps to spread cancer cells to distant sites in two ways. First, this receptor promotes cellular adhesion to the membrane-anchored version of fractalkine exposed on the surface of endothelial cells; second, CX3CR1 directs cellular migration towards concentration gradients of the soluble form of the same chemokine, which is present in most of the tissues commonly colonized by circulating tumor cells [28–30].

Our pre-clinical animal models show that breast cancer cells use the chemokine receptor CX3CR1 to seed target organs from systemic blood [31]. Interestingly, administration of CX3CR1 antagonists to animals with multiple tumors in the skeleton and soft-tissues dramatically decreased tumor burden and extended

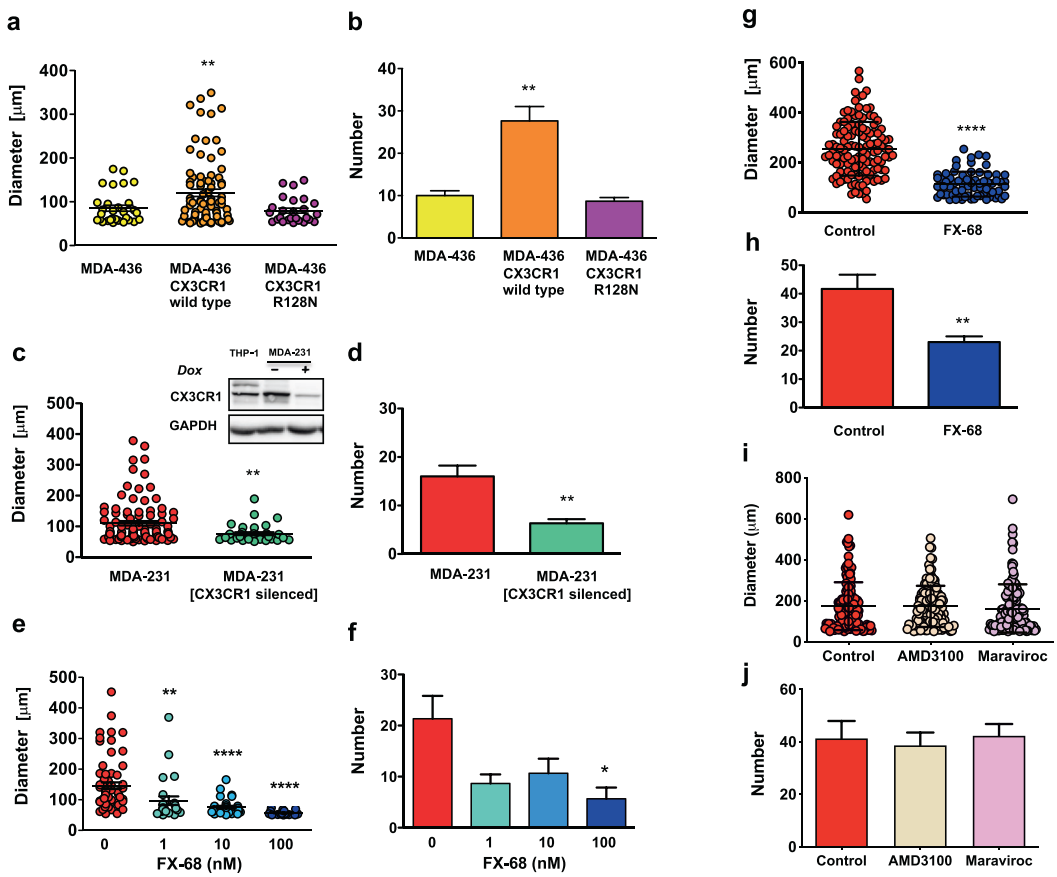

Fig. 2 Formation of tumor spheroids depends on CX3CR1 expression and signaling. The over-expression of signaling-competent CX3CR1 in MDA-436 breast cancer cells increased spheroids diameter (**a**) and number (**b**), whereas the R128N signaling-incompetent mutant did not increase either value as compared to untransfected cells. In a complementary experiment, MDA-231 breast cancer cells silenced for CX3CR1 (inset, THP-1 cells used as a positive control) showed a reduced diameter (**c**) and number (**d**) of spheroids formed in vitro. **e, f**. The CX3CR1 antagonist FX-68 inhibited spheroids formation by MDA-231 cells in a dose-dependent fashion. **g, h** Similar results were obtained with PC3-ML prostate cancer cells exposed to 100 nM FX-68**. i, j** Both AMD3100 and Maraviroc did not affect size or number of tumor spheroids in PC3-ML cells (a: $^{**}P = 0.006$; b: $^{**}P = 0.002$; c: $^{**}P = 0.003$, D: $^{*}P = 0.01$ $^{***}P < 0.0001$. Student's *t*-test or one-way ANOVA).

overall survival as compared to untreated controls [31, 32], implying a role of CX3CR1 in tumor progression. In light of these observations, we aimed to determine whether CX3CR1 identifies cancer cells with tumor-initiating potential and regulates their stemness properties, and to determine the potential of targeting this receptor for therapeutic purposes. We employed genomic, proteomic, and transcriptomic approaches to analyze cancer cells with different CX3CR1 expression either growing in vitro or harvested as DTCs from mice, tested their respective ability to grow into tumors and resist chemotherapy, defined the functional association between CX3CR1 and pluripotency genes OCT4a and NANOG and ultimately linked CX3CR1 with stemness behavior and tumor-initiating properties of breast and prostate cancer cells. Importantly, our study delineates a plausible therapeutic scenario where we can hamper metastatic progression by inactivating MICs through pharmacologic targeting of CX3CR1.

RESULTS

Primary and metastatic breast and prostate tumors harbor small contingents of cancer cells with high CX3CR1 expression

We have previously shown that conditional silencing or pharmacologic inhibition of CX3CR1 inhibited the progression of disseminated breast tumors in pre-clinical models of metastatic disease [31, 32] and have reproduced these findings in similar models of metastatic prostate cancer (in preparation). To gauge the clinical relevance of these findings, we decided to assess the presence and frequency of malignant cells that express CX3CR1 in cancer patients. To this end, we processed tissue specimens of primary and metastatic tumors for immunohistochemistry detection of CX3CR1 (Fig. 1a–d) and identified contingents of breast and prostate cancer cells that stained more intensely for this chemokine receptor than the majority of the other cancer cells inhabiting each tumor (Fig. 1e, f). The distribution of these CX3CR1^{High} cells was highly variable among specimens, ranging from a few interspersed cells (Fig. 1d) to clusters (Fig. 1b). CX3CR1^{High} cells showed co-expression of OCT4a and NANOG (Fig. 1g, h). These two transcription factors function as master regulators of pluripotency in embryonic cells [33], are silenced in normal somatic cells [34, 35] but expressed in cancer cells with stem-cell phenotypes [25]. Furthermore, they are both up regulated in breast [18] and prostate [36] cancers and have been implicated in metastasis initiation [12]. Since cells that were either CX3CR1^{Low} or negative for this receptor did not express OCT4a or NANOG, we posited that CX3CR1^{High} status would exclusively identify cancer cells with stem-like properties. To delve further into this idea, we manipulated CX3CR1 expression in human breast and prostate cancer cell lines to determine whether this receptor represents a hallmark of stemness traits.

Cancer cells with high CX3CR1 expression demonstrate stem-like properties in vitro

The ability of cancer cells to start new tumors is commonly associated with a range of properties shared with normal stem

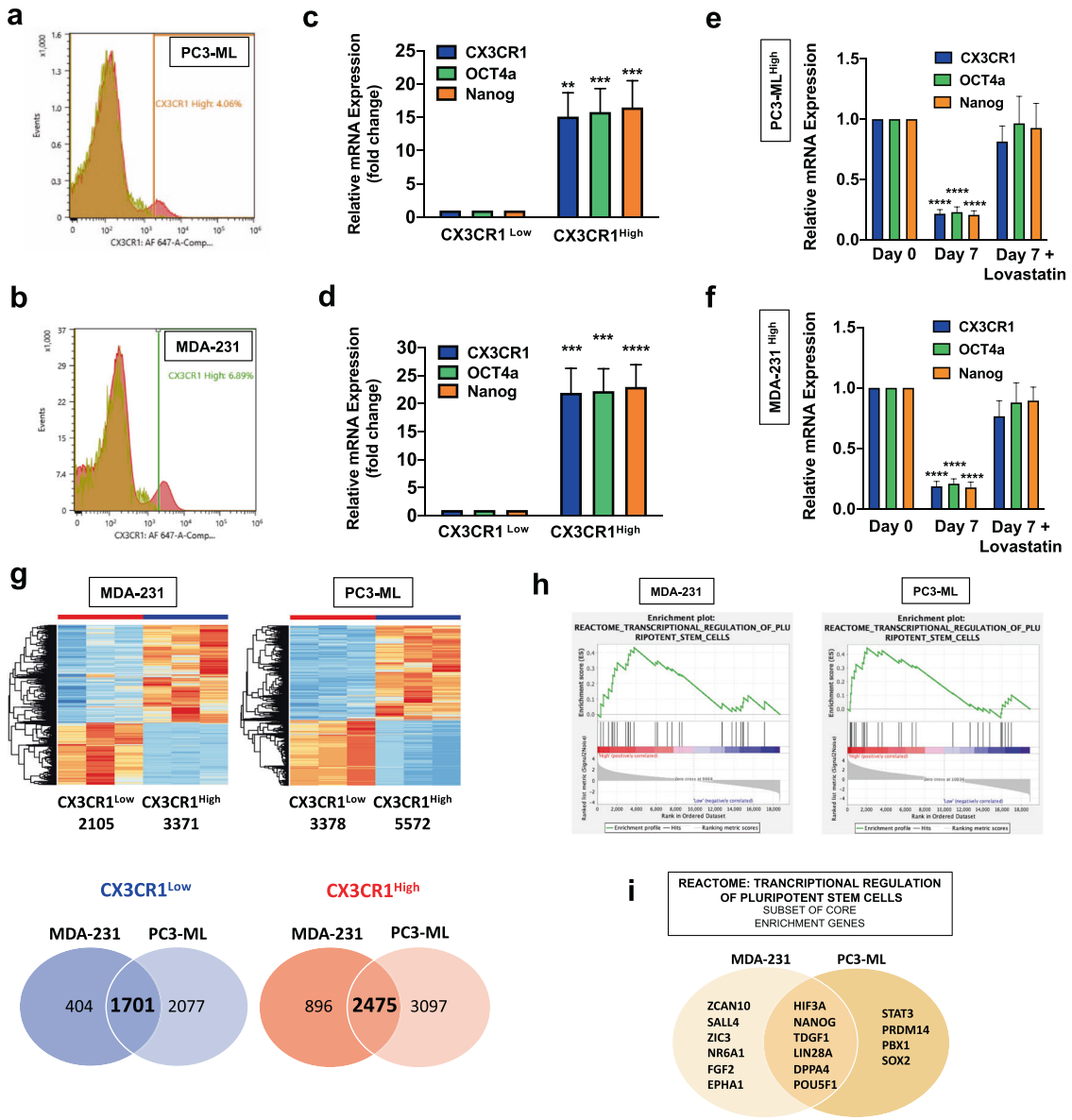

Fig. 3 Sub-populations of CX3CR1^{High} cancer cells demonstrate stemness features. Univariate histograms, obtained by flow cytometry with parental populations of PC3-ML (**a**) and MDA-231 (**b**) cells with antibodies specific for human CX3CR1, identify small contingents of cells staining for the chemokine receptor (MDA-231 cells 5±0.5% [18n] and PC3-ML 3.7±0.3% [32n]), clearly separated from the majority of each cell population that lacks CX3CR1 expression. Sorting pure CX3CR1^{Low} and CX3CR1^{High} sub-populations by FACS for transcript analysis demonstrated a significant up-regulation of CX3CR1, OCT4a, and NANOG in both PC3-ML (**c**) and MDA-231 (**d**) cells. CX3CR1^{High} cells isolated from the parental PC3-ML (**e**) and MDA-231 (**f**) cells were placed in culture for 7 days with or without 10 μM lovastatin. The transcript levels were quantified at day 7 for untreated and lovastatin treated cells and compared to the levels measured immediately after sorting (day 0). Lovastatin treatment prevented the reduction in CX3CR1, OCT4a, and NANOG transcript levels after 7 days in culture observed in untreated cells, resulting in the retention of the CX3CR1^{High} phenotype. **g** RNA-seq was performed for whole transcriptome analysis of the CX3CR1^{Low} and CX3CR1^{High} sub-populations sorted from the MDA-231 and PC3-ML parental cell lines. Differentially expressed genes are represented by a heatmap for each cell line. The number of commonly upregulated and downregulated differentially expressed genes between the MDA-231 and PC3-ML cells is represented by Venn diagrams. **h** GSEA was performed against Reactome canonical pathways and both MDA-231 and PC3-ML CX3CR1^{High} sub-populations were enriched with the transcriptional regulation of pluripotent stem cells signature. **i** The subset of core enrichment genes for both MDA-231 and PC3-ML cells contributing to the transcriptional regulation of pluripotent stem cells signature of the Reactome database. The Venn diagram shows the core enrichment genes expressed in common by CX3CR1^{High} cells sorted from MDA-231 and PC3-ML cell lines. c: $^{**}P = 0.0016$; $^{***}P = 0.0009$ (OCT4a); $^{***}P = 0.0007$ (NANOG); Nine biological replicates; d: $^{***}P = 0.0002$ (CX3CR1); $^{***}P = 0.0001$ (OCT4a); $^{****}P < 0.0001$; $n = 5$; e and f: $^{****}P < 0.0001$; g: Differentially expressed genes are defined by an adjusted p-value of ≤ 0.05 and absolute fold change of ≥ 2; H: FDR q-value = 0.0395 and NES = 1.4664 (MDA-MB-231); FDR q-value = 0.0193 and NES = 1.5932 (PC3-ML). One-way ANOVA.

cells and revealed by in vitro assays such as spheroids formation [37, 38]. Thus, we ascertained whether the expression and signaling of CX3CR1 were associated with stem-like properties of cancer cells. To this end, we first tested MDA-436 breast cancer cells engineered to exogenously over-express either wild-type CX3CR1 or its functional mutant R128N, which fails to activate downstream signaling [39]. Using low-adherence culture vessels, we found that the signaling-functional CX3CR1 promoted the

formation of larger and more numerous spheroids, whereas the R128N signaling-incompetent receptor failed to produce the same effects (Fig. 2a, b**)**. In a complementary experiment, MDA-231 breast cancer cells stably silenced for CX3CR1 by CRISPR interference [40, 41] showed a robust reduction in both diameter and number of tumor spheroids as compared to parental cells (Fig. 2c, d). Furthermore, pharmacologic inhibition of CX3CR1 by increasing concentrations of the novel and potent antagonist FX-68 [31, 32] induced a dose-dependent reduction of spheroids formation by MDA-231 cells (Fig. 2e, f). Since these cells secrete soluble fractalkine (3.0 ng/ml as measured by ELISA in vitro), the only ligand for CX3CR1 [28], it is plausible that this chemokine activates CX3CR1 in an autocrine/paracrine fashion and recruits intracellular signaling pathways that sustain spheroids formation. Notably, CX3CR1 inhibition caused similar effects in PC3-ML prostate cancer cells (Fig. 2g, h).

At least two other chemokine receptors—CXCR4 and CCR5—have been previously associated with stem-like features of tumor cells [25, 42, 43]. Therefore, to ascertain if targeting these two receptors reproduces the inhibitory effects on tumor spheroid formations by CX3CR1 antagonism, we used AMD3100 [44] and maraviroc [45] to antagonize CXCR4 and CCR5, respectively. Interestingly, we found that neither compound reduced oncosphere formation by PC3-ML cells (Fig. 2i, j) or MDA-231 cells (Supplementary Fig. 1).

Cancer cell lines harbor small, slow proliferating subpopulations with high CX3CR1 expression and upregulated pluripotency markers

Here we sought to further delineate how CX3CR1 defines the stem-like behavior and tumor-initiating properties of cancer cells. We used two different antibodies specific for human CX3CR1 with flow cytometry and cell sorting to ascertain how widespread the expression of this receptor is on the surface of MDA-231 breast cancer cells and PC3-ML prostate cancer cells. In both tumor cell lines, only small contingents of cells stained as CX3CR1^{High} phenotypes (Fig. 3a, b) and this small pool also showed up-regulation of OCT4a and NANOG (Fig. 3c, d). Notably, these findings also extended to H1703 lung cancer cells, WM793 primary melanoma cells, 1205Lu cells obtained from a lung metastasis in immunodeficient mice grafted with WM793 cells, and also in murine 4T-1 breast cancer cells (Supplementary Fig. 2). Next, we asked if increasing CX3CR1 expression is sufficient to induce OCT4a and NANOG. To this end, we examined the transcript levels of the two pluripotency genes in MDA-436 breast cancer cells over-expressing CX3CR1. We found that these cells showed a moderate but still significant up-regulation of both OCT4a and NANOG when compared to their low-CX3CR1 expressing counterparts (Supplementary Fig. 3).

CX3CR1^{High} cells also proliferate at a significantly slower rate than CX3CR1^{Low} MDA-231 and PC3-ML phenotypes, a feature previously observed in adult stem cells and also reported for CSCs [46] that further consolidates our idea of an existing link between CX3CR1 and stem-like cellular behavior (Supplementary Fig. 4a, b). As expected, CX3CR1^{High} cells were also much better equipped to migrate in vitro towards a fractalkine concentration gradient (Supplementary Fig. 4c), in line with our previous pre-clinical studies showing the crucial role played by the CX3CR1-fractaline pair in driving circulating breast and prostate cancer cells from systemic blood into target organs [31, 32].

When culturing pure CX3CR1^{High} MDA-231 breast cancer and PC3-ML prostate cancer cells for seven days following their sorting, we observed a dramatically reduced expression of the chemokine receptor and both OCT4a and NANOG, assessed by RT-qPCR on the whole population. Since MICs can divide in asymmetric fashion similarly to CSCs, we speculated that our findings revealed the ability of CX3CR1^{High} cancer cells to divide into a daughter CSC-like cell (self-renewal) and a non-CSC CX3CR1^{Low} phenotype. To corroborate this assumption, we repeated the experiment in the presence of lovastatin, a proteasome inhibitor that stabilizes the CDK inhibitors p21 and p27, which arrests cell-cycle progression at the G_1 phase [47]. We found that preclusion from cell division abolished the reduction in transcript levels for CX3CR1 and pluripotency genes in both MDA-231 and PC3-ML cells (Fig. 3e, f). Taken together, these findings nominate CX3CR1 for the first time as a putative stemness marker across cancer cells from multiple solid tumors. Based on this premise, the limited pool of cancer cells expressing CX3CR1 should display transcriptional profiles drastically different from the larger contingent of cells that lack this receptor. We tested this hypothesis using genome-wide assessment of CX3CR1-associated transcriptional networks in MDA-231 and PC3-ML cells sorted as CX3CR1^{High} and CX3CR1^{Low} pure populations and obtained consistent results among biological replicates (Supplementary Fig. 5). We detected major transcriptional variations between the two cell populations. CX3CR1^{High} cells showed 5572 up-regulated and 3778 down-regulated genes for PC3-ML cells and 3371 up-regulated and 2105 down-regulated genes for MDA-231 cells (Fig. 3g**)**. Gene set enrichment analysis (GSEA) revealed that CX3CR1 expression is associated with transcriptional programs that regulate pluripotency and stemness, including those involving OCT4a and NANOG (Fig. 3h, i), thus confirming the previous findings of this study described above.

Targeting CX3CR1 prevents tumor colonization of target organs

There is abundant evidence that spreading, proliferation and survival of cancer cells can be regulated by the chemokine system [48, 49]. We have previously reported that CX3CR1 is crucial to drive cancer cells into skeleton and soft tissues [29, 31, 32, 50, 51]. MDA-436 breast cancer cells express significantly lower levels of CX3CR1 compared to MDA-231 cells, which aggressively seed and colonize target organs when grafted *via* the intracardiac (IC) route in the systemic blood circulation of mice. The exogenous overexpression of CX3CR1 in MDA-436 cells (Fig. 4a) (also stably transduced with both GFP and Luc2 luciferase) increased their ability to seed (Fig. 4b) and conferred some tumor-initiating ability, a task at which their wild-type counterparts failed (Fig. 4c). To further underscore the role of CX3CR1 in tumor spreading and colonization, we employed FX-68, a novel and potent small-molecule antagonist of this receptor [31]. Previously, we showed that FX-68 strongly impaired the seeding of human and murine breast cancer cells [32], and here we observed the same effect using human PC3-ML prostate cancer cells (Fig. 4d). Since we could detect approximately 40% of DTCs in the bones of FX-68 treated mice compared to their untreated controls, we sought to assess if the cancer cells that seeded despite CX3CR1 blockade were endowed with tumor-initiating properties. To this end, mice received either vehicle (control group) or FX-68 prior to grafting with cancer cells via the IC route as done for the seeding experiments; however, this time we monitored animals for tumor growth over the following three weeks without any further treatment. All control mice developed tumors, as expected, whereas we detected tumors in only a minority of FX-68-treated mice (Fig. 4e). Based on these findings, we postulated that CX3CR1^{Low} cancer cells could still seed target organs upon FX-68 blockade, likely by recruiting mediators of adhesion/extravasation alternative to the CX3CR1-FKN pair, but they lacked tumor-initiating properties.

Targeting CX3CR1 prevents CX3CR1^{High} cancer cells from seeding the skeleton

Next we conducted seeding experiments in mice treated with either vehicle or FX-68 and harvested bone marrow from femora and tibiae of the animals 24 h later. We sorted cancer cells by gating for GFP signal (Fig. 5a) and evaluated them for CX3CR1

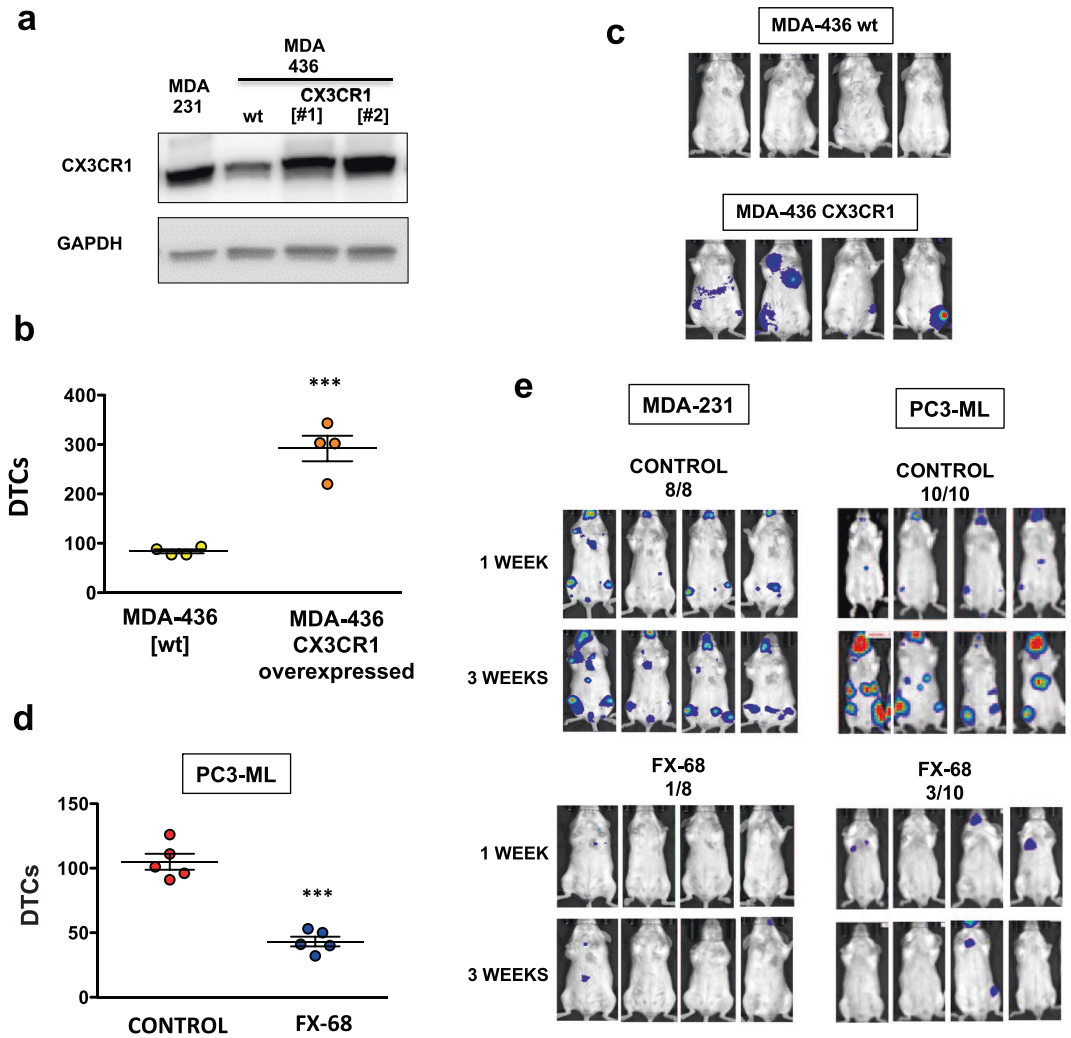

Fig. 4 CX3CR1 promotes colonization of disseminated tumor cells. Human cancer cells co-expressing GFP and Luc2 luciferase were grafted in the systemic blood circulation of mice, which were either killed 24 h later to assess tumor seeding or longitudinally monitored for tumor growth by bioluminescence imaging. a MDA-436 breast cancer cells express lower endogenous levels of CX3CR1 and are poorly metastatic. Upon over-expression of CX3CR1, MDA-436 cells were comparable to the highly metastatic MDA-231 cells, as they were more efficient in seeding the skeleton (**b**) and generated tumors in all animals, in contrast to their wild-type (wt) counterparts (**c**). **d** Mice administered with the CX3CR1 antagonist FX-68 prior to the grafting of human PC3-ML prostate cancer showed a robust reduction in tumor seeding as compared to vehicle-treated mice. **e** Animals grafted with cancer cells after receiving either vehicle or FX-68 were in vivo imaged for three weeks. Tumors were detected in all vehicle-treated control animals, whereas the CX3CR1 antagonist prevented the emergence of tumors in most of the treated animals. Four representative mice shown for each experimental group. (b: $***P = 0.0002$; 4 mice/group; d: $***P < 0.0007$; 8 mice/group in two separate experiments. Data are presented as mean values ± SEM–Student's *t*-test).

transcript levels. We found that MDA-231 and PC3-ML cells that seeded the bones of FX-68-treated mice showed much lower levels of CX3CR1 expression as compared to cells harvested from control animals. In agreement with our in vitro data, this nearly complete absence of CX3CR1 was associated with a dramatically low transcription of OCT4a and NANOG (Fig. 5b). Notably, MDA-231 and PC3-ML cancer cells harvested as DTCs from untreated animals had much higher CX3CR1 transcript expression compared to their parental populations cultured in vitro (Fig. 5c). This dramatic enrichment confirms that the skeleton is predominantly targeted by CX3CR1^{High} phenotypes, in line with our previous work and consistent with the seeding data shown above (Fig. 4d).

CX3CR1^{High} phenotypes are uniquely capable of initiating disseminated tumors

Collectively, the findings reported above strongly suggest that disseminated tumors were reduced in FX-68 treated mice (Fig. 4e) by preventing CX3CR1^{High} cells from seeding target organs. Further GSEA analyses revealed that high CX3CR1 expression was associated with genes and enrichment of pathways widely implicated in regulating stemness behavior (Fig. 5d, e). Thus, to determine whether CX3CR1^{High} phenotypes are endowed with tumor-initiating behavior, we grafted mice subcutaneously with PC3-ML cells sorted as pure populations of either CX3CR1^{High} (1×10^4 cells) or CX3CR1^{Low} (1×10^5 cells) cells. When normalized for cell numbers at grafting, CX3CR1^{High} cells generated larger tumors than their CX3CR1^{Low} counterparts (Supplementary Fig. 6). However, to establish whether high CX3CR1 expression was associated with metastasis-initiating potential of cells seeding target organs, we delivered cancer cells to mice *via* IC route, including pure CX3CR1^{High} or CX3CR1^{Low} cells (2.5×10^4) sorted from either PC3-ML or MDA-231 cells. After monitoring animals by in vivo bioluminescence imaging, we found that 9 mice grafted with CX3CR1^{High} cells developed tumors out of the 14 mice

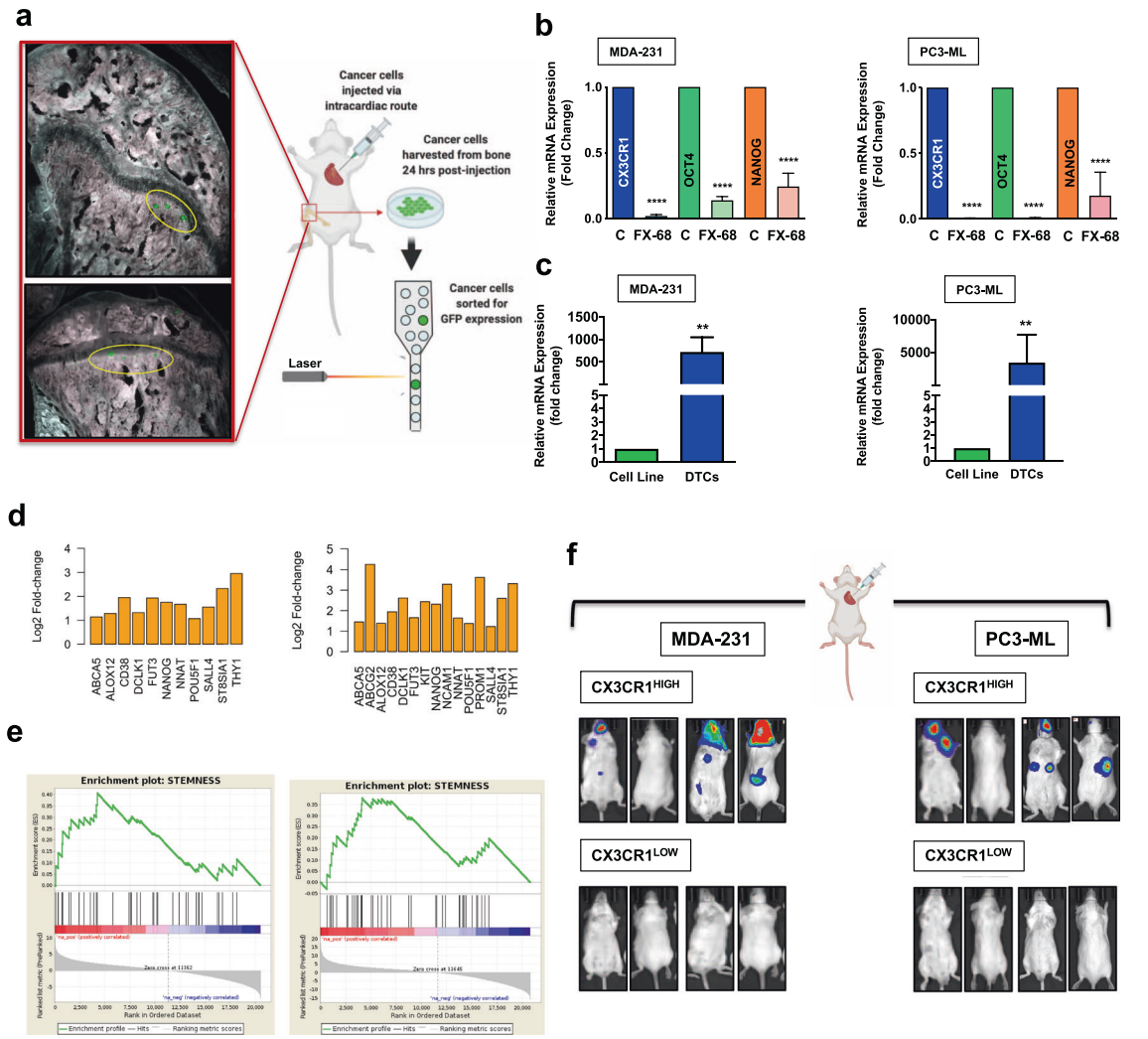

Fig. 5 CX3CR1^{High} cells are tumor-initiating. a MDA-231 parental cells co-expressing GFP and Luc2 luciferase or PC3-ML parental cells co-expressing mCherry and RedLuc luciferase were injected via intracardiac route in mice, allowing for systemic dissemination. Mice were treated with either vehicle or FX-68 (100 nM), prior to injection of cancer cells. Animals were sacrificed after 24 h and DTCs from the knee-joints collected by tissue dissociation and FACS based on GFP or mCherry expression, and analyzed for CX3CR1, OCT4a, and NANOG transcripts. **b** Compared to control animals receiving vehicle, both MDA-231 and PC3-ML DTCs from mice treated with FX-68 had significantly lower levels of CX3CR1, OCT4a, and NANOG transcripts as compared to control animals. **c** The levels of CX3CR1 transcript in DTCs isolated from animals that received vehicle was significantly higher than the levels detected in the parental MDA-231 and PC3-ML cell lines grown in culture, indicating an enrichment in CX3CR1^{High} cells seeding the skeleton from systemic circulation. **d** GSEA performed using the CSCdb showed that CX3CR1^{High} cells of both MDA-231 and PC3-ML lines were enriched for the stemness signature and revealed an overlap of the subset of core enrichment genes contributing to the CSCdb signature between CX3CR1^{High} cells and TICs (**e**). **f** 1 x 10^4 CX3CR1^{High} cells or 1 10^5 CX3CR1^{Low} cells, sorted from MDA-231 parental cells expressing GFP and Luc2 luciferase (left) and 2.5 × 10^4 CX3CR1^{High} cells or 2.5 × 10^4 CX3CR1^{Low} cells, sorted from PC3-ML parental cells co-expressing RedLuc luciferase and mCherry (right), were injected into mice via intracardiac route. Animals were monitored weekly (MDA-231: 12 weeks; PC3-ML: 6 weeks) for tumor development and progression using bioluminescence imaging. Nine out of 14 total mice injected with CX3CR1^{High} cells developed tumors. One out of 12 total mice injected with CX3CR1^{Low} cells developed a single tumor. Four representative mice shown for each experimental group. (c: ****$P < 0.0001$ (MDA-231); ****$P < 0.0001$ (PC3-ML); c: **$P = 0.02$ (MDA-231); **$P = 0.01$ (PC3-ML); d: FDR q-value = 0.0229 and NES = 1.5498 (MDA-231); FDR q-value = 0.0308 and NES = 1.4398 (PC3-ML). One-way ANOVA or Ratio paired t-test).

injected (Fig. 5f). In contrast, we could detect only one tumor in the 12 mice injected with CX3CR1^{Low} PC3-ML cells. Notably, this tumor could only be detected at the 3rd week post-grafting, in contrast to just one week needed for tumors generated by CX3CR1^{High} cells to become evident by in vivo bioluminescence imaging.

To rule out the possibility that these findings could result from a CX3CR1^{Low} sub-population harboring cells with a CX3CR1-expressing phenotype, we confirmed the accuracy of our procedure by performing two sequential sorting sessions, which confirmed the extremely high purity of the two sub-populations for both cell lines used. (Supplementary Figs. 7 and 8**)**.

CX3CR1^{Low} cells undergo phenotypic plasticity in vitro

Differentiated phenotypes could represent transient states; indeed, predictive models and experimental evidence support the concept that non-CSCs may shift to a CSC state [21, 52, 53]. Therefore, we sought to ascertain whether CX3CR1^{Low} cells, which based on our findings we identify as non-CSC phenotypes, could give rise to CX3CR1^{High} cells. Thus, we cultured pure populations

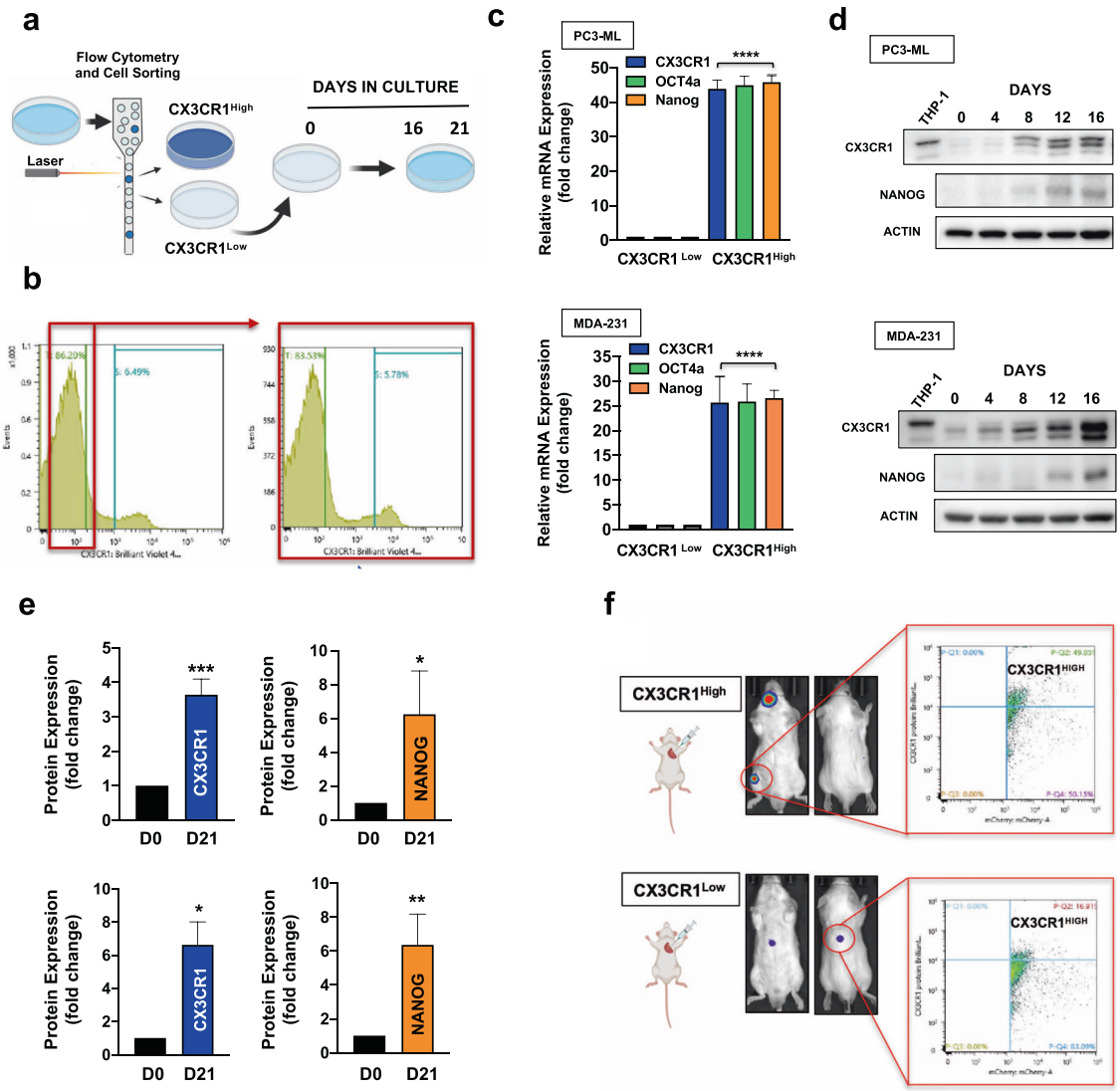

Fig. 6 CX3CR1^{Low} cells exhibit phenotypic plasticity. a CX3CR1^{Low} cells were sorted from MDA-231 and PC3-ML parental cell lines and placed in culture for 16 days (western blotting) or 21 days (flow cytometry, FACS, transcript analysis, and western blotting). **b** After 21 days the cultures that started as CX3CR1^{Low} pure cells showed the re-emergence of CX3CR1^{High} phenotypes, assessed by flow cytometry. The newly generated CX3CR1^{High} cells were isolated by FACS and, when the transcript levels of CX3CR1, OCT4a, and NANOG were quantified, they showed significantly higher levels of all three transcripts as compared to the CX3CR1^{Low} cells (**c**). **d** CX3CR1^{Low} cells were isolated from MDA-231 and PC3-ML parental cells and placed in culture for 16 days and cell lysates collected every four days. Western blotting analysis showed that in these conditions CX3CR1 re-expression occurred between 4 and 8 days of culture, while NANOG protein started being re-expressed between 8 and 12 days of culture. THP-1, a human monocytic cell line, served as a positive control for CX3CR1 protein detection. **e** The increase in CX3CR1 and NANOG protein levels was assessed by densitometry and compared between CX3CR1^{Low} cells immediately after sorting and after 21 days in culture. **f** The tumors generated from intracardiac inoculation of CX3CR1^{Low} and CX3CR1^{High} cells sorted from PC3-ML parental line were dissociated for flow cytometry analysis of CX3CR1 cell-surface expression. The single skeletal tumor generated by pure CX3CR1^{Low} cells harbored 17% of CX3CR1^{High} cells, indicating the occurrence of phenotypic plasticity in vivo. The skeletal tumors generated by pure CX3CR1^{High} cells contained higher fractions of CX3CR1^{High} phenotypes (35±4%) as compared to the parental cell line cultured in vitro (*see* Fig. 3). (c: ****$P < 0.0001$ (MDA-231); ****$P < 0.0001$ (*P*C3-ML); e: ***P = 0.0005; *$P = 0.03$ (Top: PC3-ML); *$P = 0.01$; **$P = 0.007$ (Bottom: MDA-231). One-way ANOVA or Student's *t*-test).

of sorted CX3CR1^{Low} MDA-231 or PC3-ML cells in vitro for 21 days (Fig. 6a). Each cell population was then sorted again by gating for CX3CR1 surface expression, and we used RT-qPCR to assess transcript levels. The results showed that CX3CR1^{Low} cells reconstituted the phenotypic patterns of both MDA-231 and PC3-ML parental cell lines, harboring fractions of CX3CR1^{High} cells comparable to those detected in the unsorted populations (Fig. 6b). As expected, the CX3CR1^{High} phenotypes that emerged from pure CX3CR1^{Low} cells also upregulated OCT4a and NANOG (Fig. 6c). These findings were further corroborated by cultures of pure CX3CR1^{Low} cells that were sampled at different time-points. We found that the protein levels of CX3CR1 and NANOG progressively increased over time (Fig. 6d, e).

CX3CR1^{High} cells divide asymmetrically and CX3CR1^{Low} cells undergo phenotypic plasticity in vivo

When we harvested cells from tumors generated by pure populations of CX3CR1^{High} cells grafted via IC route in mice, they consistently showed CX3CR1-mixed phenotypes (Fig. 6f, top). This finding is in line with the expected generation of CX3CR1^{Low} cells

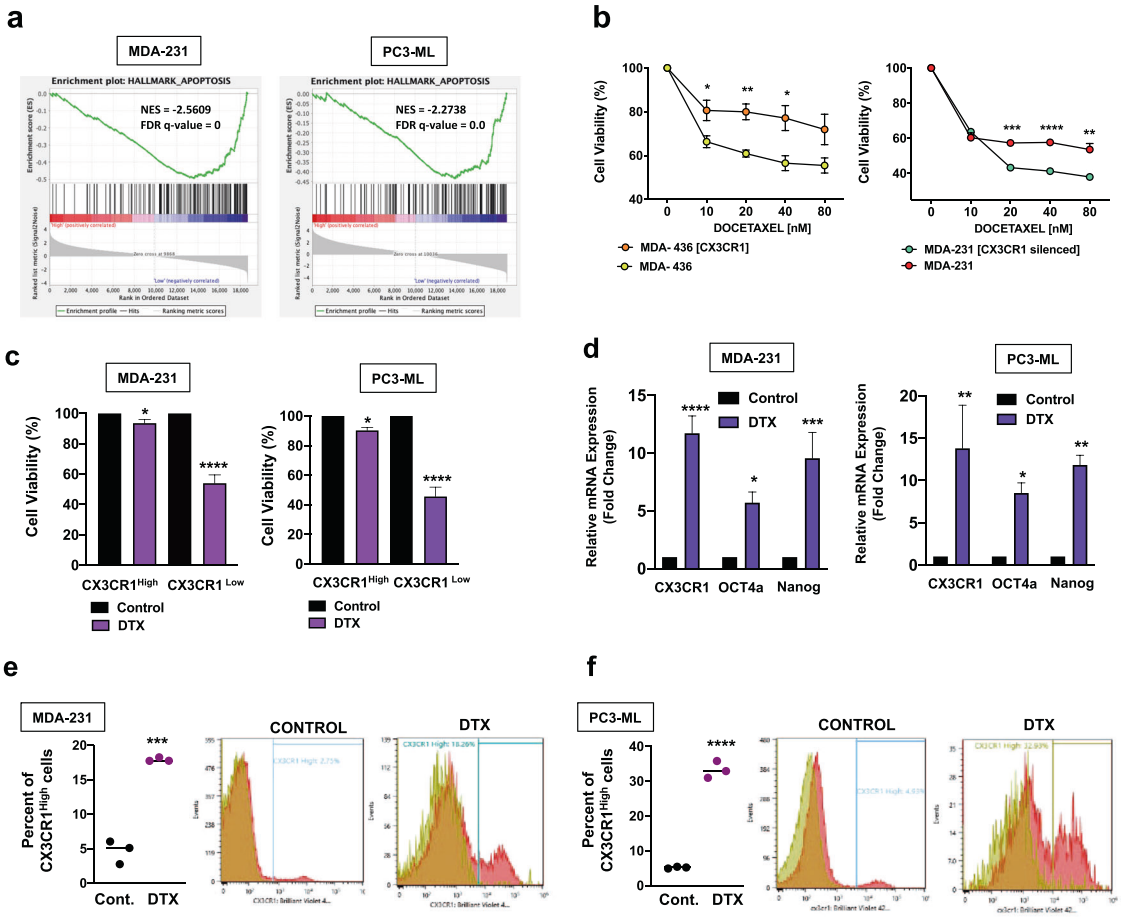

Fig. 7 CX3CR1^{High} cells show resistance to docetaxel. a GSEA was performed on Hallmark canonical pathways and both the MDA-231 and PC3-ML CX3CR1^{High} sub-populations were de-enriched of the apoptosis signature. **b** MDA-436 cells either wild-type or over-expressing CX3CR1 were treated with the indicated doses of docetaxel for 72 h and assessed for cell viability. MDA-436 cells over-expressing CX3CR1 were significantly less sensitive to docetaxel than wild-type cells. MDA-231 wild-type cells and MDA-231 cells with CX3CR1 silenced by CRISPRi were treated with the indicated doses of docetaxel for 72 hours and cell viability was assessed. MDA-231 cells with CX3CR1 silenced were significantly more sensitive to docetaxel than wild-type cells. **c** CX3CR1^{Low} and CX3CR1^{High} sub-populations isolated by FACS from MDA-231 and PC3-ML parental cells were treated with 20 nM docetaxel for 72 h, and cell viability was compared to the respective untreated population. Both MDA-231 and PC3-ML CX3CR1^{Low} cells showed significantly lower cell viability with docetaxel treatment. **d** PC3-ML parental cells were treated with 20 nM docetaxel for 10 days and MDA-231 parental cells were treated with 100 nM docetaxel for 5 days. The surviving populations of cells were collected for quantification of CX3CR1, OCT4a, and NANOG mRNA. Compared to the untreated controls, the MDA-231 and PC3-ML cells treated with docetaxel had significantly higher levels of CX3CR1, OCT4a, and NANOG transcripts. **e, f** The MDA-231 and PC3-ML cells that survived docetaxel treatment were collected for analysis of CX3CR1 cell-surface expression by flow cytometry. In comparison to untreated cells, the MDA-231 and PC3-ML cells surviving docetaxel treatment harbored significantly larger CX3CR1^{High} sub-populations. (a: FDR q-value = 0.0 and NES = −2.5609 (MDA-231); FDR q-value = 0.0 and NES = −2.2738 (PC3-ML); b: $^{*}P = 0.038$; $^{**}P = 0.003$; $^{*}P = 0.02$ (left); $^{***}P = 0.0002$; $^{****}P < 0.0001$; $^{**}P = 0.005$ (right); c: $^{*}P = 0.01$; $^{****}P < 0.0001$; $n = 6$/data point (MDA-231); $^{*}P = 0.02$; $^{****}P < 0.0001$; $n = 4$/data point (PC3-ML); d: $^{****}P < 0.0001$; $^{***}P < 0.0004$; $^{*}P = 0.0154$ (MDA-231); $^{*}P = 0.04$; $^{**}P = 0.002$ (CX3CR1); $^{**}P = 0.005$ (NANOG) (PC3-ML); e: $^{***}P = 0.0002$; F: $^{****}P < 0.0001$. One-way ANOVA or Student's t-test).

by asymmetric division of CX3CR1^{High} cells following their seeding of target organs, thus replicating ours in vitro results.

If the phenotypic plasticity we observed in vitro also occurs in vivo, then CX3CR1^{Low} cells that transition into a CX3CR1^{High} status could re-acquire tumor-initiating potential and generate tumors in tissues. Strikingly, we found that the only tumor harvested from mice grafted with CX3CR1^{Low} cells harbored CX3CR1-mixed populations (Fig. 6f, bottom). This indicates that CX3CR1^{High} subsets could indeed re-surface from a uniformly CX3CR1^{Low} cell population by undergoing non-CSC phenotypic plasticity, an occurrence for which evidence is constantly emerging [19, 20, 22, 54].

Finally, and irrespective of the initiating CX3CR1 phenotype, all analyzed tumors harbored fractions of CX3CR1^{High} cells higher than what we measured in the same cells cultured in vitro.

CX3CR1 expression reduces susceptibility of cancer cells to docetaxel

Resistance to chemotherapy is a crucial feature of CSCs and MICs [55, 56]. Our GSEA analysis revealed that CX3CR1^{High} cells showed a de-enrichment of the apoptosis signature (Fig. 7a). Therefore, we asked whether CX3CR1 could affect the susceptibility of cancer cells to the cytotoxic effects of docetaxel, a chemotherapeutic drug that is currently standard of care for breast and prostate cancers [57–59]. We first over-expressed CX3CR1 in MDA-436 cells and observed a significant increase in the resistance of these cells to increasing concentrations of docetaxel (Fig. 7b). Then, we used CRISPRi technology to target CX3CR1 in MDA-231 cells, as previously described [31], and observed that suppressing the expression of the receptor made these cells more susceptible to the drug (Fig. 7b). These initial results suggested that docetaxel

killed most CX3CR1^{Low} cells but largely spared CX3CR1^{High} phenotypes. To support this paradigm, we treated pure populations of CX3CR1^{High} or CX3CR1^{Low} cells sorted from MDA-231 or PC3-ML parental lines with 20 nM docetaxel for 72 hours and confirmed that CX3CR1^{Low} cells were exceedingly more susceptible to the cytotoxic effects of docetaxel (Fig. 7c). Consistently, we treated parental MDA-231 cells with 100 nM docetaxel and PC3-ML cells with 20 nM docetaxel for 5 and 10 days, respectively, based on previously defined killing curves for each cell type (not shown). We found that the surviving cells dramatically upregulated the transcription of CX3CR1, OCT4a, and NANOG (Fig. 7d), making a compelling case for the positive selection of CX3CR1^{High} cells following docetaxel exposure. We further corroborated these findings by flow cytometry, which confirmed a robust enrichment in CX3CR1^{High} MDA-231 and PC3-ML cells as compared to each untreated cell type (Fig. 7e, f).

DISCUSSION

In the present study, we report the crucial findings that CX3CR1 is detected in breast and prostate cancer cells that display stemness features, and its expression is directly associated with tumor-initiating behavior. This new information is of high clinical relevance, since it is widely recognized that only a true minority of cancer cells can give rise to new tumors, should they be dislodged to different organ sites. These rare malignant cells share molecular and functional features with normal stem cells and are appropriately designated as MICs based on their ability to generate new secondary lesions and amplify metastatic burden. MICs also play a key role when confined within a tumor mass by generating highly proliferating non-CSCs responsible for rapid growth, while preserving their small cellular pool by self-renewing in response to cell-intrinsic mechanisms and stroma-derived factors.

We have previously shown that targeting CX3CR1 by molecular or pharmacological means strongly impairs tumor seeding in animal models of metastatic disease. Interestingly, CX3CR1 inactivation also significantly reduced the growth of established secondary tumors, which could not be attributed to the inhibition of adhesion and migration of cancer cells. Thus, based on this preclinical evidence, we posited that CX3CR1 could also promote tumor progression and decided to delineate the expression patterns of this receptor in breast and prostate cancer patients. First, we examined tissues from skeletal metastases and found small contingents of tumor cells that expressed high levels of CX3CR1, while the remaining majority expressed much lower levels of the receptor, if any. We observed a similar scenario in tissues from primary prostate and breast adenocarcinomas. When quantified, these CX3CR1^{High} cells were variable among different metastatic and primary tumors but were consistently underrepresented compared to CX3CR1^{Low} cells within each tumor specimen examined. Most importantly, the co-expression of CX3CR1 and the embryonal pluripotency genes OCT4a and NANOG provided the first indication that CX3CR1 could identify prostate and breast malignant phenotypes endowed with stem-cell like features. The limited number of patient's samples assessed in this study did not allow us to draw conclusions about possible correlations between the fraction of CX3CR1^{High} cells detected and each of the different molecular sub-types currently recognized for prostate and breast tumors. Nevertheless, it is unprecedented that all examined lesions, both primary and metastatic, harbored rare cells that uniquely co-expressed CX3CR1, OCT4a and NANOG.

Previous work has reported a connection between CX3CR1 signaling and the establishment and progression of solid tumors. In addition to our own work [31, 32, 51], others have proposed this receptor can activate pro-tumorigenic pathways in cancer cells of the pancreas [60], ovary [61, 62], lung [63], and glioblastoma [64, 65], among others. Interestingly, The Cancer Genome Atlas (TCGA) did not report any significant association between CX3CR1 expression and patients' overall survival (OS), except for ovarian cancer (HR: 1.37, 95% CI: 1.05, $P = 0.02$; data not shown). These results should be expected considering the paucity of CX3CR1^{High} cells we detected within each tumor mass and the unavoidable harvesting of non-tumor tissues and stroma-derived RNA when developing genomic databases, as also emphasized in another recent study [66]. This confounding factor is particularly limiting when the goal is to probe non-mutated genes that encode for proteins widely expressed by normal tissues, such as CX3CR1. Therefore, future studies must be tailored to the specific need of dissecting and interrogating rare tumor cells with putative stemness features to effectively establish a direct link between MICs that inhabit individual tumors and the related patients' clinical outcomes.

We also observed that CX3CR1 upregulation or silencing in cancer cells altered their formation of tumor spheroids, an in vitro assay widely used to assess the potential for self-renewal and stemness features of sub-populations of cancer cell lines. Our results showed that in MDA-231 breast and PC3-ML prostate cancer cells CX3CR1 expression strongly promotes the formation of tumor spheroids. Notably, this receptor must be signaling competent to exert this effect, as shown by the experiments in which cancer cells were engineered to express a CX3CR1 functional mutant incapable of recruiting downstream pathways. The potential to pharmacologically inhibit CX3CR1 to target cells with stem-cell like properties was substantiated by using FX-68, which impaired tumor spheroids in a dose-dependent manner and provided results in agreement with the functional IC_{50} for this compound as we previously reported [32]. Our group and others have shown that CX3CR1 activates multiple signaling pathways in tumor cells, including PI3K/AKT [29, 67], Raf/MEK/ERK [31, 68], and JAK/STAT [69, 70], among others. We are currently conducting studies to systematically assess how distinct signaling pathways sustain the stemness behavior of CX3CR1^{High} cells.

To further corroborate the existence of CX3CR1^{High} phenotypes with stemness properties, we sorted cell lines from several solid tumors for sub-populations of tumor cells that co-expressed the embryonal genes OCT4a and NANOG. We observed a consistent, direct correlation between CX3CR1 and these recognized markers of pluripotency and self-renewal among cells from tumors of both human and murine origin, which is a unique finding. To date, several putative or established cell surface CSCs protein markers have been reported [25]; however, only CD44 and CD133 are highly expressed across several types of tumors. Our study places CX3CR1 in this restricted group of surface markers with the unique property of identifying CSC in multiple malignancies.

After seven days in culture following their sorting as pure CX3CR1^{High} cells, the whole population showed significantly decreased expression of CX3CR1, OCT4a, and NANOG, which we attributed to the generation of CX3CR1^{Low} phenotypes by asymmetric division. This central stemness feature of CX3CR1^{High} cells was confirmed by pharmacologically impeding cell cycle progression, which preserved both CX3CR1 and pluripotency genes expression. Genomic analyses by RNA sequencing clearly segregated CX3CR1^{High} and CX3CR1^{Low} cells based on distinct transcriptomic profiles. In both breast MDA-231 and prostate PC3-ML cancer cells, CX3CR1 expression corresponded with enrichment in pathways regulating pluripotency and stemness. A subset of core enrichment genes identified OCT4a and NANOG – thus confirming our RT-qPCR results–along with several other genes over-expressed in both cell lines and warranting further studies to dissect their respective roles in conferring stem-cell like properties.

Taken together, these findings lend support to the idea that CX3CR1^{High} cells are endowed with tumor-initiating properties and could therefore behave as MICs. Indeed, the exogenous over-expression of CX3CR1 in MDA-436 breast cancer cells conferred

moderate tumor-initiating behavior in mice, suggesting this receptor helps to sustain initial colonization and progression following seeding of target organs. To corroborate this idea, we administered the CX3CR1 antagonist FX-68 to mice prior to intracardiac grafting of cancer cells. The dramatic reduction of disseminated tumors in FX-68 treated animals, combined with the impaired tumor seeding, strongly pointed to the depletion of CX3CR1-expressing, tumor-initiating phenotypes in target organs as the cause of hampered metastatic behavior.

On the other hand, in this and previous studies [32], we found that a percentage of tumor cells could seed the skeleton despite FX-68 treatment; we interpret this finding as the result of the expression and functional intervention of molecular mediators of cellular adhesion and extravasation alternative to CX3CR1. These mediators include integrins β1 [71] and αvβ3 [72, 73], intracellular adhesion molecule 1 (ICAM-1) [74], cell adhesion molecule 1 (LCAM-1) [75] and several selectins [76, 77], among many others [78], which have all been implicated in tumor seeding. Similarly, chemokine receptors such as CXCR4 [79–81] and CCR5 [82] have been proposed to help drive tumor cells migration towards selected tissues. However, we posit that some or all these molecules could be comparably expressed by cells capable and incapable of tumor-initiation. This possibility seems likely, based on the absence of tumor spheroid impairment in both MDA-231 and PC3-ML cells treated with either CXCR4 or CCR5 antagonists and the similar RNA-Seq profiles for CXCR4 and CCR5 we detected in CX3CR1^{High} and CX3CR1^{Low} phenotypes (Data available in NCBI GEO). Our studies also show that the skeleton is predominantly seeded by CX3CR1^{High} phenotypes, which were enriched several fold as compared to unsorted MDA-231 and PC3-ML populations. Thus, to further support the role of CX3CR1 in stemness and tumor-initiating behavior, we conducted GSEA on the cancer stem cell database (CSCdb), which was generated from more than 13,000 articles identifying more than 1,700 genes as implicated in the functional regulation of CSCs [83]. We found that CX3CR1^{High} cells from both MDA-231 and PC3-ML populations were highly enriched for many genes in the CSCdb signature, including ABCA5 (ATP-binding cassette A5), a membrane transporter upregulated in prostate cancer [84] and involved in cholesterol trafficking, indicating an involvement in both lipid metabolism and androgen/estrogen hormone synthesis [85, 86]. Also enriched was DCLK1 (doublecortin-like kinase 1), a kinase that regulates self-renewal and epithelial-mesenchymal transition (EMT) in CSCs of the breast, prostate, and other solid tumors [87]. Further, we found enrichment of SALL4, a transcriptional and epigenetic modulator suppressed in most adult tissues [88] that is involved in OCT4a and NANOG expression [89, 90], can reprogram somatic cells into pluripotent stem cells [88, 91, 92] and binds the murine promoter of CX3CR1 [93]. The latter finding lends support to the idea that SALL4 could regulate the transcription of human CX3CR1, thus controlling the switch between the two CX3CR1-expressing states. These transcriptomic analyses prompted us to assess the tumor-initiating abilities of CX3CR1^{High} cells as the pure population in vivo. The subcutaneous grafting of CX3CR1^{High} cells in mice generated significantly larger tumors than those observed in animals grafted with CX3CR1^{Low} cells. However, although widely adopted, this model does not test for metastatic behavior and fails to consider the selective pressure applied on tumor cells by distinctively diverse tissue microenvironments. To address these crucial points, we delivered pure CX3CR1^{High} and CX3CR1^{Low} cells, separately and via IC route, into animals longitudinally monitored for tumor growth by in vivo bioluminescence imaging. In this model, cancer cells arrive to skeleton and soft-tissues from the systemic blood circulation as either single units or few-cells aggregates, thus facing the same conditions encountered when spreading to target organs in patients. When tested in this model, CX3CR1^{High} cells were the only phenotype that could generate tumors. These results indicate that CX3CR1 expression identifies the rare cells with a metastasis-initiating phenotype and allows us to separate them from their cellular counterparts, a much larger contingent lacking both this receptor and stem-cell like properties, including tumor-initiation.

Over the years, the identification of CSCs consolidated the view that these cells would divide in an asymmetric fashion and self-renew, thereby serving as the sole source for their lineage. This led to the paradigm of a unidirectional, hierarchic process by which the terminally differentiated tumor cells generated by CSCs would not be able to de-differentiate. However, recent evidence supports the concept of *phenotypic plasticity*, by which cell-intrinsic and environmental signals can induce differentiated cancer cells to switch back to a CSC state [54, 94]. In addition to promoting tumor heterogeneity, phenotypic plasticity could potentially undermine the current impetus towards the development of strategies for targeting CSCs in the clinic [55, 95]. Indeed, if CSCs were generated from non-CSCs, their complete eradication could eventually elude our efforts in the long term. For instance, even if differentiated tumor cells are more sensitive to cytotoxic and targeted therapies, their ablation might not be achieved prior to the conversion of a fraction of surviving cells into CSCs due to incomplete penetration of most drugs in solid tumors [96]. This would refuel tumor growth and lead to further tumor recurrences [22]. Therefore, decoding the molecular and temporal terms of phenotypic plasticity is of utmost importance for understanding tumor progression and conceiving more effective therapies.

In this study, we addressed this issue by sorting pure CX3CR1^{Low} cells from MDA-231 breast cancer and PC3-ML prostate cancer cell lines and culturing them in vitro for 21 days. Upon finding the reconstitution of a CX3CR1^{High} sub-population over time, we considered the possibility that these cells had contaminated the CX3CR1^{Low} population during sorting. However, we detected only 0.09% of PC3-ML cells and 0.04% of MDA-231 cells, in each respective CX3CR1^{Low} re-sorted population; since CX3CR1^{High} cells are slowly proliferating as compared to their CX3CR1^{Low} counterparts, it is unlikely that they could be primarily responsible for the reconstituted CX3CR1^{High} population we detected. Thus, taken together, these observations suggest that CX3CR1^{Low} phenotypes can switch back to a CX3CR1^{High} state, which also entails re-expression of OCT4a and NANOG. This appears to be a gradual process, as shown by the progressive increase in CX3CR1 and NANOG protein products assessed in CX3CR1^{Low} cells in culture that were sampled at regular intervals following their sorting and plating. Intriguingly, the re-expression of CX3CR1 appeared to precede that of NANOG, tempting us to envision this receptor located upstream of the signaling pathways that regulate pluripotency genes; this is also in light of the increase in OCT4a and NANOG transcription in MDA-436 cells engineered to exogenously over-express CX3CR1. Notably, OCT4a and NANOG have been reported as downstream targets of the JAK/STAT pathway [97, 98], which can be recruited by CX3CR1 in tumor cells [60, 99]. Further studies will be necessary to tease out the reciprocal molecular and functional interactions that may connect CX3CR1 downstream signaling with transcriptional regulation of OCT4a, NANOG, and possibly other PPGs.

Phenotypic plasticity has been previously related to the occurrence of EMT and—at least for breast and pancreatic adenocarcinomas – the intervention of the transcription factor Zeb 1 [100, 101]. For breast cancer in particular, Zeb1 was reported as being 10-fold over-expressed in CD44^{HI} cells, which are widely recognized as endowed with stem-like properties and tumor-initiating potential [94, 100, 102, 103]. We found no differences in either CD44 or Zeb1 expression between CX3CR1^{High} and CX3CR1^{Low} phenotypes sorted from both MDA-231 and PC3-ML cells (data available in NCBI GEO). However, the transcription profiles of several other EMT-related genes significantly differed in relation to CX3CR1 expression and for both cell lines, indicating that EMT-related signaling pathways were enriched in CX3CR1^{High} cells (Supplementary Fig. 9).

We found evidence that phenotypic plasticity also occurs in vivo, as shown by one mouse out of the twelve that we grafted with pure CX3CR1^{Low} cells developing a tumor that harbored a cancer population with mixed CX3CR1-expressing status. Interestingly, the CX3CR1^{High} fraction represented almost 17% of the entire population of cancer cells inhabiting the tumor, in contrast to the ~3-5% subsets commonly observed in both MDA-231 and PC3-ML cells tested either unsorted or following re-constitution in culture starting from pure CX3CR1^{Low} populations. This provides compelling evidence that the rate of transition between CSC and non-CSC states is influenced by microenvironmental factors within the tumor niche [104, 105]. We find it interesting that the only tumor generated by pure CX3CR1^{Low} cells became detectable by bioluminescence imaging three weeks after IC grafting, in contrast to only one week needed by tumors generated by pure CX3CR1^{High} cells. This points to the plausibly longer time needed by non-CSC CX3CR1^{Low} phenotypes to undergo plasticity and acquire tumor-initiating abilities as compared to tumors generated by pure CX3CR1^{High} cells. The fact that this process became evident in only one of the twelve animals similarly grafted with CX3CR1^{Low} cells implies that a series of complex and still unidentified mechanisms regulate phenotypic plasticity in vivo. These mechanisms likely affect the behavior of CX3CR1^{High} cells as well, as suggested by the much higher percentage of these cells isolated from tumors in animals as compared to the respective unsorted parental populations. A likely and intriguing explanation for this finding is that CSCs generate two CSC daughter cells in the presence of appropriate tissue conditions more often than when grown in culture, thereby increasing their pool.

An additional and extremely interesting finding of our RNA Seq analyses was the de-enrichment in pathways involved in cell death and caspase activation in CX3CR1^{High} cells. We used GSEA to interrogate the *Hallmark* gene set collection, which is based on the original Molecular Signature database (MSigDB [106]) and condenses information across multiple gene sets by highlighting genes with coordinate expression and represented in well-defined biological processes [107]. The *Apoptosis* gene set, containing 161 genes, provided unequivocal evidence that high CX3CR1 expression was significantly correlated with a lower propensity to undergo cell death (FRD q-value = 0). A key property of CSC is their resistance to cytotoxic insults, including those delivered by chemotherapeutics. This creates an insurmountable obstacle to the eradication of tumors, particularly for metastatic patients, as the initial success in ablating most of the tumor mass will leave behind drug-resistant cells that will resume growth, eventually leading to patients' demise. Based on this premise, we first showed that CX3CR1 expression protects breast cancer cells from the cytotoxic effects of docetaxel in vitro. This initial observation was complemented by the finding that >50% of CX3CR1^{Low} cells sorted from the MDA-231 and PC3-ML cell lines were killed by docetaxel, whereas the viability of their CX3CR1^{High} counterparts was only minimally affected. Taken together, these results suggest that CX3CR1^{High} cells are much more likely to survive a longer exposure to cytotoxic agents and eventually be positively selected from the more susceptible CX3CR1^{Low} cells. Preliminary evidence in support of this idea was provided by experiments in which MDA-231 and PC3-ML cells were exposed as unsorted populations to docetaxel for 10 or 5 days in vitro, respectively, and analyzed for CX3CR1, OCT4a, and NANOG transcription. The dramatic increase in expression for all three genes suggested that the surviving cells in both populations were enriched in CX3CR1^{High} phenotypes. This notion was confirmed by flow cytometry of MDA-231 and PC3-ML CX3CR1^{High} cells. Even though both cell types have some intrinsic resistance to apoptosis (MDA-231 breast cancer cells harbor a mutated p53 [108] and PC3-ML cells are null for this tumor suppressor [109]), our results clearly show that CX3CR1 expression independently confers an additional, strong refractory advantage to the cytotoxicity caused by docetaxel. Since a large spectrum of chemotherapeutics and targeted therapies relies on apoptosis to kill tumor cells [110–112], it is plausible that CX3CR1^{High} cells can resist the effect of drugs additional to docetaxel, thus contributing to the treatment resistance commonly experienced in clinical settings.

In conclusion, we have identified the chemokine receptor CX3CR1 as a marker of stem-cell properties and metastasis-initiating behavior and shown that CX3CR1^{High} cells can be detected both in the prostate and breast cancer patients and human and murine cell lines from multiple solid tumors. Furthermore, we found CX3CR1 associated with distinct transcriptional profiles that overlap with known signatures for stemness and apoptosis resistance. Cancer cells lacking both CX3CR1 and the stemness and tumor-initiating properties induced by its expression and signaling can switch to a CX3CR1^{High} status both in vitro and in vivo, implying that CSCs can be continuously generated under appropriate microenvironmental conditions. Since CX3CR1^{High} cells can sustain and/or refuel tumor growth and resist cell death, this observation presents high clinical relevance and should contribute to a paradigm shift in the current therapeutic approaches for patients with solid tumors. Finally, our study provides conceptual ground for the development of compounds targeting CSCs by inactivating CX3CR1. This strategy, combined with systemic therapies reducing the bulk of non-CSCs, should have the highest likelihood of eradicating metastatic tumors.

MATERIALS AND METHODS

Cell lines and cell cultures

Human MDA-MB-231 (MDA-231) and MDA-MB-436 (MDA-436) breast cancer cells, human H1703 lung cancer cells, and murine 4T-1 breast cancer cells were purchased from ATCC. The human PC3-ML prostate cancer cell line was derived from the parental PC3 cells as previously described [113]. These cell lines were cultured in DMEM (Gibco)—except the 4T-1 cells that were cultured in RPMI (Gibco) - supplemented with 10% fetal bovine serum (FBS, HyClone) and 0.1% gentamicin (Gibco). The human WM793 melanoma cell line and the 1205Lu cell line, derived from a lung metastasis induced in immunocompromised mice grafted with WM793 cells, were a gift from Dr. Edward Hartsough (Pharmacology and Physiology, Drexel University). Cell line authentication was performed by IDEXX BioResearch using a single tandem repeat and conducted to determine the species of origin and rule out interspecies contamination by performing the *CellCheck 9 Plus* test. All cell lines were also tested for Mycoplasma contamination by IDEXX on a regular basis using PCR detection and only negative cells were used for this study. See further details in Supplementary Methods.

Tumorsphere formation assay, SDS-Page and western blotting, chemotaxis, and cell proliferation assay

They are detailed in Supplementary Methods.

Flow cytometry and sorting, and CX3CR1 cell-surface staining

We used an SH-800 Cell Sorter (Sony Biotechnology) with a 130 µm microfluidic sorting chip. Prior to sample acquisition and sorting, single-cell suspensions were obtained using a 70 µm cell strainer (Bel-Art SP Scienceware Flowmi). Further details are available in Supplementary Methods.

In vitro treatment with docetaxel or lovastatin

MDA-231 and PC3-ML parental cells were plated for 24 h to a final confluency of 90%. MDA-231 cells were treated with 100 nM docetaxel (LC Laboratories) for 5 days, with fresh docetaxel-containing media added on day 3 of treatment. PC3-ML cells were treated with 20 nM docetaxel for 10 days, with fresh docetaxel-containing media added every 3 days. Following treatment, cells were washed twice with PBS to remove dead cells prior to RNA isolation or flow cytometry, conducted as described elsewhere. For lovastatin treatment, MDA-231 and PC3-ML cells were stained for CX3CR1 cell-surface expression and CX3CR1^{High} cells were sorted, using ultra-purity sorting mode, into DMEM supplemented with

10% FBS. Cells were plated for both control and lovastatin treatment for collection at days 0 and 7. Cells were allowed to attach overnight prior to treatment. Lovastatin (Selleckchem) was used at a concentration of 10 μM, with fresh lovastatin-containing media added every 3 days. Cells were lysed with buffer RLT directly in the culture dish, and RNA was isolated using the RNeasy Mini Kit (Qiagen).

Intracardiac injection of tumor cells

This procedure was performed as in [51] and is further detailed in Supplementary Methods. All in vivo experiments were performed in accordance with NIH guidelines for the humane use of animals. All protocols involving the use of animals were approved by the Drexel University College of Medicine Committee for the Use and Care of Animals.

Processing of mouse tissues for enumeration, fluorescence microscopy, and FACS analysis of DTCs and tumors

These procedures were performed as in [31, 32, 114] and are detailed in Supplementary Methods.

Subcutaneous grafting of cancer cells

PC3-ML cells (1×10^4 $CX3CR1^{High}$ and 1×10^5 $CX3CR1^{Low}$) were grafted in the flank of 6-week old male C.B. 17 SCID mice (Charles River), using an insulin syringe and by delivering a 100μl suspension containing 30% Matrigel. Animals were weekly monitored for tumor growth by in vivo bioluminescence imaging as described above and sacrificed at 6 weeks post-grafting. Photon counting recorded for each mouse was normalized to the number of cancer cells injected and expressed as tumor burden.

Gene expression analysis by RT-qPCR and RNA-Sequencing

They are detailed in Supplementary methods.

Patient-derived samples and immunohistochemistry staining

De-identified paraffin-embedded sections from patients with metastatic prostate cancer and metastatic breast cancer were obtained from the Sidney Kimmel Cancer Center Biorepository of Thomas Jefferson University, a College of American Pathologists (CAP)-accredited biorepository (accreditation # 8427654), with support from the Cancer Center Grant 5P30CA056036-21. Acquisition of the biospecimens was approved through Thomas Jefferson University under IRB #16P.726. Specificity of the primary antibodies used was validated as shown in Supplementary Figure 10 and further details are provided in Supplementary Methods.

Statistical analysis

All in vitro and in vivo experiments were analyzed using Prism 9.0 (Graph Pad Software). For comparison between two groups, a Student *t*-test with Welch's correction was used assuming no equal variance. For comparisons between more than two groups, a one-way ANOVA was performed. Ratio-pared *t* test was used when required by the experiment and as indicated. In vitro experiments were repeated at least three times. In vivo experiments were conducted with at least two cohorts of animals per treatment/data point.

DATA AVAILABILITY

RNA-Seq data have been deposited in the NCBI GEO with the submission code PRJNA736860.

Molecular Signature database (MSigDB) and gene set enrichment analysis were utilized for pathways analyses.

REFERENCES

1. Miller KD, Nogueira L, Mariotto AB, Rowland JH, Yabroff KR, Alfano CM, et al. Cancer treatment and survivorship statistics, 2019. CA Cancer J Clin. 2019;69:363–85.
2. Ganesh K, Massagué J. Targeting metastatic cancer. Nat Med. 2021;27:34–44.
3. Riihimäki M, Thomsen H, Sundquist K, Sundquist J, Hemminki K. Clinical landscape of cancer metastases. Cancer Med. 2018;7:5534–42.
4. Dillekås H, Rogers MS, Straume O. Are 90% of deaths from cancer caused by metastases? Cancer Med-US. 2019;8:5574–6.
5. Massagué J, Obenauf AC. Metastatic colonization by circulating tumour cells. Nature. 2016;529:298–306.
6. Ignatiadis M, Georgoulias V, Mavroudis D. Micrometastatic disease in breast cancer: clinical implications. Eur J Cancer. 2008;44:2726–36.
7. Riethdorf S, Wikman H, Pantel K. Review: Biological relevance of disseminated tumor cells in cancer patients. Int J Cancer J Int DU Cancer. 2008;123:1991–2006.
8. Obenauf AC, Massagué J. Surviving at a distance: organ specific metastasis. Trends Cancer. 2015;1:76–91.
9. Micalizzi DS, Maheswaran S, Haber DA. A conduit to metastasis: circulating tumor cell biology. Genes Dev. 2017;31:1827–40.
10. Chaffer CL, Weinberg RA. A perspective on cancer cell metastasis. Science. 2011;331:1559–64.
11. Zhang W, Bado IL, Hu J, Wan Y-W, Wu L, Wang H, et al. The bone microenvironment invigorates metastatic seeds for further dissemination. Cell. 2021;184:2471–2486.e20.
12. Celià-Terrassa T, Kang Y. Distinctive properties of metastasis-initiating cells. Genes Dev. 2016;30:892–908.
13. Celià-Terrassa T, Kang Y. Metastatic niche functions and therapeutic opportunities. Nat Cell Biol. 2018;20:868–77.
14. Esposito M, Kang Y. Targeting tumor–stromal interactions in bone metastasis. Pharmacol Ther. 2014;141:222–33.
15. Zhou H, Neelakantan D, Ford HL. Clonal cooperativity in heterogenous cancers. Semin Cell Dev Biol. 2017;64:79–89.
16. Liu A, Yu X, Liu S. Pluripotency transcription factors and cancer stem cells: small genes make a big difference. Chin J Cancer. 2013;32:483–7.
17. Wang Y-J, Herlyn M. The emerging roles of Oct4 in tumor-initiating cells. Am J Physiol- Cell Physiol. 2015;309:C709–18.
18. Ben-Porath I, Thomson MW, Carey VJ, Ge R, Bell GW, Regev A, et al. An embryonic stem cell-like gene expression signature in poorly differentiated aggressive human tumors. Nat Genet. 2008;40:499–507.
19. Batlle E, Clevers H. Cancer stem cells revisited. Nat Med. 2017;23:1124–34.
20. Cabrera MC, Hollingsworth RE, Hurt EM. Cancer stem cell plasticity and tumor hierarchy. World J Stem Cells. 2015;7:27–36.
21. Gupta PB, Pastushenko I, Skibinski A, Blanpain C, Kuperwasser C. Phenotypic plasticity: driver of cancer initiation, progression, and therapy resistance. Cell Stem Cell. 2018;24:65–78.
22. Chen W, Dong J, Haiech J, Kilhoffer M-C, Zeniou M. Cancer stem cell quiescence and plasticity as major challenges in cancer therapy. Stem Cells Int. 2016;2016:1–16.
23. Das PK, Pillai S, Rakib MDA, Khanam JA, Gopalan V, Lam AKY, et al. Plasticity of cancer stem cell: origin and role in disease progression and therapy resistance. Stem Cell Rev Rep. 2020;16:397–412.
24. Qureshi-Baig K, Ullmann P, Haan S, Letellier E. Tumor-initiating cells: a critical review of isolation approaches and new challenges in targeting strategies. Mol Cancer. 2017;16:40.
25. Zhao W, Li Y, Zhang X. Stemness-related markers in cancer. Cancer Transl Med. 2017;3:87–95.
26. Walcher L, Kistenmacher A-K, Suo H, Kitte R, Dluczek S, Strauß A, et al. Cancer stem cells—origins and biomarkers: perspectives for targeted personalized therapies. Front Immunol. 2020;11:1280.
27. Morein D, Erlichman N, Ben-Baruch A. Beyond cell motility: the expanding roles of chemokines and their receptors in malignancy. Front. Immunol. 2020;11:952.
28. Imai T, Hieshima K, Haskell C, Baba M, Nagira M, Nishimura M, et al. Identification and molecular characterization of fractalkine receptor CX3CR1, which mediates both leukocyte migration and adhesion. Cell. 1997;91:521–30.
29. Shulby S, Dolloff N, Stearns M, Meucci O, Fatatis A. CX3CR1-fractalkine expression regulates cellular mechanisms involved in adhesion, migration, and survival of human prostate cancer cells. Cancer Res. 2004;64:4693–8.
30. Fong A, Robinson L, Steeber D, Tedder T, Yoshie O, Imai T, et al. Fractalkine and CX3CR1 mediate a novel mechanism of leukocyte capture, firm adhesion, and activation under physiologic flow. J Exp Med. 1998;188:1413.
31. Shen F, Zhang Y, Jernigan DL, Feng X, Yan J, Garcia FU, et al. Novel small-molecule CX3CR1 antagonist impairs metastatic seeding and colonization of breast cancer cells. Mol Cancer Res: MCR. 2016;14:518–27.
32. Qian C, Worrede-Mahdi A, Shen F, DiNatale A, Kaur R, Zhang Q, et al. Impeding circulating tumor cell reseeding decelerates metastatic progression and potentiates chemotherapy. Mol Cancer Res: MCR. 2018;16:1844–54.
33. Boyer LA, Lee TI, Cole MF, Johnstone SE, Levine SS, Zucker JP, et al. Core transcriptional regulatory circuitry in human embryonic stem cells. Cell. 2005;122:947–56.
34. Shi G, Jin Y. Role of Oct4 in maintaining and regaining stem cell pluripotency. Stem Cell Res Ther. 2010;1:39.
35. Kim J, Liu Y, Qiu M, Xu Y. Pluripotency factor Nanog is tumorigenic by deregulating DNA damage response in somatic cells. Oncogene. 2016;35:1334–40.
36. Gu G, Yuan J, Wills M, Kasper S. Prostate cancer cells with stem cell characteristics reconstitute the original human tumor in vivo. Cancer Res. 2007;67:4807–15.

37. Gassenmaier M, Chen D, Buchner A, Henkel L, Schiemann M, Mack B, et al. CXC chemokine receptor 4 is essential for maintenance of renal cell carcinoma-initiating cells and predicts metastasis. Stem Cells. 2013;31:1467–76.
38. Lombardo Y, Giorgio A de, Coombes CR, Stebbing J, Castellano L. Mammosphere formation assay from human breast cancer tissues and cell lines. *J. Vis. Exp.* 2015. https://doi.org/10.3791/52671.
39. Haskell CA, Cleary MD, Charo IF. Molecular uncoupling of fractalkine-mediated cell adhesion and signal transduction. Rapid flow arrest of CX3CR1-expressing cells is independent of G-protein activation. J Biol Chem. 1999;274:10053–8.
40. Stojic L, Lun ATL, Mangei J, Mascalchi P, Quarantotti V, Barr AR, et al. Specificity of RNAi, LNA and CRISPRi as loss-of-function methods in transcriptional analysis. Nucleic Acids Res. 2018;46:5950–66.
41. Mandegar MA, Huebsch N, Frolov EB, Shin E, Truong A, Olvera MP, et al. CRISPR interference efficiently induces specific and reversible gene silencing in human iPSCs. Cell Stem Cell. 2016;18:541–53.
42. Kucia M, Reca R, Miekus K, Wanzeck J, Wojakowski W, Janowska-Wieczorek A, et al. Trafficking of normal stem cells and metastasis of cancer stem cells involve similar mechanisms: pivotal role of the SDF-1-CXCR4 Axis. Stem Cells. 2005;23:879–94.
43. Jiao X, Nawab O, Patel T, Kossenkov AV, Halama N, Jaeger D, et al. Recent advances targeting CCR5 for cancer and its role in immuno-oncology. Cancer Res. 2019;79:4801–7.
44. Hatse S, Princen K, Bridger G, Clercq ED, Schols D. Chemokine receptor inhibition by AMD3100 is strictly confined to CXCR4. FEBS Lett. 2002;527:255–62.
45. Dorr P, Westby M, Dobbs S, Griffin P, Irvine B, Macartney M, et al. Maraviroc (UK-427,857), a potent, orally bioavailable, and selective small-molecule inhibitor of chemokine receptor CCR5 with broad-spectrum anti-human immunodeficiency virus type 1 activity. Antimicrobial Agents Chemother. 2005;49:4721–32.
46. Cheung TH, Rando TA. Molecular regulation of stem cell quiescence. Nat Rev Mol Cell Biol. 2013;14:329–40.
47. JavanMoghadam-Kamrani S, Keyomarsi K. Synchronization of the cell cycle using Lovastatin. Cell Cycle. 2008;7:2434–40.
48. Mantovani A, Savino B, Locati M, Zammataro L, Allavena P, Bonecchi R. The chemokine system in cancer biology and therapy. Cytokine Growth Factor Rev. 2010;21:27–39.
49. Kakinuma T, Hwang ST. Chemokines, chemokine receptors, and cancer metastasis. J Leukoc Biol. 2006;79:639–51.
50. Jamieson WL, Shimizu S, D'Ambrosio JA, Meucci O, Fatatis A. CX3CR1 is expressed by prostate epithelial cells and androgens regulate the levels of CX3CL1/fractalkine in the bone marrow: potential role in prostate cancer bone tropism. Cancer Res. 2008;68:1715–22.
51. Jamieson-Gladney WL, Zhang Y, Fong AM, Meucci O, Fatatis A. The chemokine receptor CX3CR1 is directly involved in the arrest of breast cancer cells to the skeleton. Breast Cancer Res: BCR. 2011;13:1584.
52. Gupta PB, Fillmore CM, Jiang G, Shapira SD, Tao K, Kuperwasser C, et al. Stochastic state transitions give rise to phenotypic equilibrium in populations of cancer. Cells Cell. 2011;146:633–44.
53. Yuan S, Norgard RJ, Stanger BZ. Cellular plasticity in cancer. Cancer Discov. 2019;9:837–51.
54. Thankamony AP, Saxena K, Murali R, Jolly MK, Nair R. Cancer Stem cell plasticity – a deadly deal. *Fronti. Mol. Biosci.* 2020; 7: 79.
55. Annett S, Robson T. Targeting cancer stem cells in the clinic: current status and perspectives. Pharmacol Ther. 2018;187:13–30.
56. Quayle LA, Ottewell PD, Holen I. Chemotherapy resistance and stemness in mitotically quiescent human breast cancer cells identified by fluorescent dye retention. Clin Exp Metastasis. 2018;35:831–46.
57. King KM, Lupichuk S, Baig L, Webster M, Basi S, Whyte D, et al. Optimal use of taxanes in metastatic breast cancer. Curr Oncol. 2009;16:8–20.
58. Palmeri L, Vaglica M, Palmeri S. Weekly docetaxel in the treatment of metastatic breast cancer. Ther Clin Risk Manag. 2008;4:1047–59.
59. Agarwal N, Lorenzo GD, Sonpavde G, Bellmunt J. New agents for prostate cancer. Ann Oncol. 2014;25:1700–9.
60. Huang L, Ma B, Ma J, Wang F. Fractalkine/CX3CR1 axis modulated the development of pancreatic ductal adenocarcinoma via JAK/STAT signaling pathway. Biochem Biophys Res Commun. 2017;493:1510–7.
61. Kim M, Rooper L, Xie J, Kajdacsy-Balla AA, Barbolina MV. Fractalkine receptor CX(3)CR1 is expressed in epithelial ovarian carcinoma cells and required for motility and adhesion to peritoneal mesothelial cells. Mol Cancer Res: MCR. 2012;10:11–24.
62. Main HG, Xie J, Muralidhar GG, Elfituri O, Xu H, Kajdacsy-Balla AA *et al*. Emergent role of the fractalkine axis in dissemination of peritoneal metastasis from epithelial ovarian carcinoma. *Oncogene*. 2016. https://doi.org/10.1038/onc.2016.456.
63. Liu Y, Ma H, Dong T, Yan Y, Sun L, Wang W. Clinical significance of expression level of CX3CL1–CX3CR1 axis in bone metastasis of lung cancer. *Clin Transl Oncol*. 2020; 1–11.
64. Locatelli M, Boiocchi L, Ferrero S, Martinelli Boneschi F, Zavanone M, Pesce S, et al. Human glioma tumors express high levels of the chemokine receptor CX3CR1. Eur Cytokine Netw. 2010;21:27–33.
65. Erreni M, Solinas G, Brescia P, Osti D, Zunino F, Colombo P, et al. Human glioblastoma tumours and neural cancer stem cells express the chemokine CX3CL1 and its receptor CX3CR1. Eur J Cancer. 2010;46:3383–92.
66. Francescone R, Vendramini-Costa DB, Franco-Barraza J, Wagner J, Muir A, Lau AN, et al. Netrin G1 promotes pancreatic tumorigenesis through cancer-associated fibroblast–driven nutritional support and immunosuppression. Cancer Discov. 2021;11:446–79.
67. Yao X, Qi L, Chen X, Du J, Zhang Z, Liu S. Expression of CX3CR1 associates with cellular migration, metastasis, and prognosis in human clear cell renal cell carcinoma. Urol Oncol: Semin Original Investig. 2014;32:162–70.
68. Lee S-J, Namkoong S, Kim Y-M, Kim C-K, Lee H, Ha K-S, et al. Fractalkine stimulates angiogenesis by activating the Raf-1/MEK/ERK- and PI3K/Akt/eNOS-dependent signal pathways. Am J Physiol-heart C. 2006;291:H2836–H2846.
69. Wada A, Ito A, Iitsuka H, Tsuneyama K, Miyazono T, Murakami J, et al. Role of chemokine CX3CL1 in progression of multiple myeloma via CX3CR1 in bone microenvironments. Oncol Rep. 2015;33:2935–9.
70. LaFave LM, Levine RL. JAK2 the future: therapeutic strategies for JAK-dependent malignancies. Trends Pharm Sci. 2012;33:574–82.
71. Kato H, Liao Z, Mitsios JV, Wang H-Y, Deryugina EI, Varner JA, et al. The primacy of β1 integrin activation in the metastatic cascade. PLoS One. 2012;7:e46576.
72. Weber MR, Zuka M, Lorger M, Tschan M, Torbett BE, Zijlstra A, et al. Activated tumor cell integrin αvβ3 cooperates with platelets to promote extravasation and metastasis from the blood stream. Thrombosis Res. 2016;140:S27–S36.
73. Zheng DQ, Woodard AS, Fornaro M, Tallini G, Languino LR. Prostatic carcinoma cell migration via alpha(v)beta3 integrin is modulated by a focal adhesion kinase pathway. Cancer Res. 1999;59:1655–64.
74. Huh SJ, Liang S, Sharma A, Dong C, Robertson GP. Transiently entrapped circulating tumor cells interact with neutrophils to facilitate lung metastasis development. Cancer Res. 2010;70:6071–82.
75. Er EE, Valiente M, Ganesh K, Zou Y, Agrawal S, Hu J, et al. Pericyte-like spreading by disseminated cancer cells activates YAP and MRTF for metastatic colonization. Nat Cell Biol. 2018;20:966–78.
76. Geng Y, Marshall JR, King MR. Glycomechanics of the metastatic cascade: tumor cell-endothelial cell interactions in the circulation. Ann Biomed Eng. 2012;40:790–805.
77. Bendas G, Borsig L. Cancer cell adhesion and metastasis: selectins, integrins, and the inhibitory potential of heparins. Int J Cell Biol. 2012;2012:676731–10.
78. Worrede A, Meucci O, Fatatis A. Limiting tumor seeding as a therapeutic approach for metastatic disease. *Pharmacol Ther* 2019. https://doi.org/10.1016/j.pharmthera.2019.03.007.
79. Ramsey DM, McAlpine SR. Halting metastasis through CXCR4 inhibition. Bioorg Med Chem Lett. 2013;23:20–25.
80. Mukherjee D, Zhao J. The Role of chemokine receptor CXCR4 in breast cancer metastasis. Am J Cancer Res. 2013;3:46–57.
81. Gravina GL, Mancini A, Muzi P, Ventura L, Biordi L, Ricevuto E, et al. CXCR4 pharmacogical inhibition reduces bone and soft tissue metastatic burden by affecting tumor growth and tumorigenic potential in prostate cancer preclinical models. Prostate. 2015;75:1227–46.
82. Singh SK, Mishra MK, Eltoum I-EA, Bae S, Lillard JW, Singh R. CCR5/CCL5 axis interaction promotes migratory and invasiveness of pancreatic cancer cells. Sci Rep. 2018;8:1323.
83. Shen Y, Yao H, Li A, Wang M. CSCdb: a cancer stem cells portal for markers, related genes and functional information. *Database* 2016; 2016: baw023.
84. Karatas OF, Guzel E, Duz MB, Ittmann M, Ozen M. The role of ATP-binding cassette transporter genes in the progression of prostate cancer. Prostate. 2016;76:434–44.
85. Pasello M, Giudice AM, Scotlandi K. The ABC subfamily A transporters: multifaceted players with incipient potentialities in cancer. Semin Cancer Biol. 2019;60:57–71.
86. Chimento A, Casaburi I, Avena P, Trotta F, Luca AD, Rago V, et al. Cholesterol and its metabolites in tumor growth: therapeutic potential of statins in cancer treatment. Front Endocrinol. 2019;9:807.
87. P Chadrakesan, J Panneerselvam. Regulatory roles of Dclk1 in epithelial mesenchymal transition and cancer stem cells. *J Carcinog Mutagen.* 2016; 2016. https://doi.org/10.4172/2157-2518.1000257.
88. Tatetsu H, Kong NR, Chong G, Amabile G, Tenen DG, Chai L. SALL4, the missing link between stem cells, development and cancer. Gene. 2016;584:111–9.
89. Yang J, Gao C, Chai L, Ma Y. A Novel SALL4/OCT4 transcriptional feedback network for pluripotency of embryonic stem cells. Plos One. 2010;5:e10766.
90. Yang J. SALL4 as a transcriptional and epigenetic regulator in normal and leukemic hematopoiesis. Biomark Res. 2018;6:1.
91. Rao S, Roumiantsev S, McDonald L, Orkin SH. The role Of Sall4 in embryonic stem cell pluripotency. Biol Blood Marrow Tr. 2010;16:S187.

92. Tsubooka N, Ichisaka T, Okita K, Takahashi K, Nakagawa M, Yamanaka S. Roles of Sall4 in the generation of pluripotent stem cells from blastocysts and fibroblasts. Genes Cells. 2009;14:683–94.
93. Yang J, Chai L, Fowles TC, Alipio Z, Xu D, Fink LM, et al. Genome-wide analysis reveals Sall4 to be a major regulator of pluripotency in murine-embryonic stem cells. Proc Natl Acad Sci. 2008;105:19756–61.
94. Chaffer CL, Brueckmann I, Scheel C, Kaestli AJ, Wiggins PA, Rodrigues LO, et al. Normal and neoplastic nonstem cells can spontaneously convert to a stem-like state. Proc Natl Acad Sci. 2011;108:7950–5.
95. Pützer BM, Solanki M, Herchenröder O. Advances in cancer stem cell targeting: how to strike the evil at its root. Adv Drug Deliv Rev. 2017;120:89–107.
96. Minchinton AI, Tannock IF. Drug penetration in solid tumours. Nat Rev Cancer. 2006;6:583–92.
97. Do DV, Ueda J, Messerschmidt DM, Lorthongpanich C, Zhou Y, Feng B, et al. A genetic and developmental pathway from STAT3 to the OCT4-NANOG circuit is essential for maintenance of ICM lineages in vivo. Genes Dev. 2013;27:1378–90.
98. Kim S-Y, Kang JW, Song X, Kim BK, Yoo YD, Kwon YT, et al. Role of the IL-6-JAK1-STAT3-Oct-4 pathway in the conversion of non-stem cancer cells into cancer stem-like cells. Cell Signal. 2013;25:961–9.
99. Yang XP, Mattagajasingh S, Su S, Chen G, Cai Z, Fox-Talbot K, et al. Fractalkine upregulates intercellular adhesion molecule-1 in endothelial cells through CX3CR1 and the Jak Stat5 pathway. Circulation Res. 2007;101:1001–8.
100. Chaffer CL, Marjanovic ND, Lee T, Bell G, Kleer CG, Reinhardt F, et al. Poised chromatin at the ZEB1 promoter enables breast cancer cell plasticity and enhances tumorigenicity. Cell. 2013;154:61–74.
101. Krebs AM, Mitschke J, Losada ML, Schmalhofer O, Boerries M, Busch H, et al. The EMT-activator Zeb1 is a key factor for cell plasticity and promotes metastasis in pancreatic cancer. Nat Cell Biol. 2017;19:518–29.
102. Al-Hajj M, Wicha MS, Benito-Hernandez A, Morrison SJ, Clarke MF. Prospective identification of tumorigenic breast cancer cells. Proc Natl Acad Sci USA. 2003;100:3983–8.
103. Li W, Ma H, Zhang J, Zhu L, Wang C, Yang Y. Unraveling the roles of CD44/CD24 and ALDH1 as cancer stem cell markers in tumorigenesis and metastasis. Sci Rep.-UK. 2017;7:13856.
104. Zhao Y, Dong Q, Li J, Zhang K, Qin J, Zhao J, et al. Targeting cancer stem cells and their niche: perspectives for future therapeutic targets and strategies. Semin Cancer Biol. 2018;53:139–55.
105. Pein M, Insua-Rodríguez J, Hongu T, Riedel A, Meier J, Wiedmann L, et al. Metastasis-initiating cells induce and exploit a fibroblast niche to fuel malignant colonization of the lungs. Nat Commun. 2020;11:1494.
106. Liberzon A, Subramanian A, Pinchback R, Thorvaldsdóttir H, Tamayo P, Mesirov JP. Molecular signatures database (MSigDB) 3.0. Bioinformatics. 2011;27:1739–40.
107. Liberzon A, Birger C, Thorvaldsdóttir H, Ghandi M, Mesirov JP, Tamayo P. The molecular signatures database hallmark gene set collection. Cell Syst. 2015;1:417–25.
108. Olivier M, Eeles R, Hollstein M, Khan MA, Harris CC, Hainaut P. The IARC TP53 database: new online mutation analysis and recommendations to users. Hum Mutat. 2002;19:607–14.
109. Carroll AG, Voeller HJ, Sugars L, Gelmann EP. p53 oncogene mutations in three human prostate cancer cell lines. Prostate. 1993;23:123–34.
110. Hanahan D, Weinberg RA. The hallmarks of cancer. Cell. 2000;100:57–70.
111. Hanahan D, Weinberg RA. Hallmarks of cancer: the next generation. Cell. 2011;144:646–74.
112. Holohan C, Schaeybroeck SV, Longley DB, Johnston PG. Cancer drug resistance: an evolving paradigm. Nat Rev Cancer. 2013;13:714–26.
113. Wang M, Stearns ME. Isolation and characterization of PC-3 human prostatic tumor sublines which preferentially metastasize to select organs in S.C.I.D. mice. Differ Res Biol Divers 1991;48:115–25.
114. Shahriari K, Shen F, Worrede-Mahdi A, Liu Q, Gong Y, Garcia FU, et al. Cooperation among heterogeneous prostate cancer cells in the bone metastatic niche. Oncogene. 2017;36:2846–56.

ACKNOWLEDGEMENTS

This work was supported by NCI grant R01-CA202929 (AF and OM), DoD grant BC150659 (AF), Wallace H. Coulter Foundation (AF and OM), Pennsylvania Breast Cancer Coalition (AF), Exceptional Project Grant from Breast Cancer Alliance (AF), and the Sidney Kimmel Cancer Center (SKCC) Support Grant 5P30CA056036-21 (AF). We would like to thank: Dr. Meenhard Herlyn (Wistar Institute, Philadelphia, PA) and Dr. Edward Hartsough (Pharmacology and Physiology, Drexel University College of Medicine) for providing the WM793 and 1205Lu human melanoma cell lines; Dr. Edward Hartsough (Pharmacology and Physiology, Drexel University College of Medicine) and Dr. Josep Domingo-Domenech (Cancer Biology, SKCC at Thomas Jefferson University) for helpful discussions; Dr. Paolo Fortina, Professor of Cancer Biology and Director of the Cancer Genomics and Translational Research/Pathology core services at SKCC for consultation and advice with RNA Sequencing; Ms. Shannon Cremin (Translational Research Project Manager), Ms. Danielle Wentworth (Biorepository Manager) and the SKCC Biorepository of Thomas Jefferson University for providing the human specimens used in this study. The authors are also grateful to Dr. Bradley Nash (Director, Office of Scientific Communications, Department of Pharmacology and Physiology, Drexel University College of Medicine) for critically reading and editing the manuscript.

AUTHOR CONTRIBUTIONS

AD: Conceptualization, investigation, data generation (molecular biology, biochemistry, flow cytometry and cell sorting, cell culturing and in vitro treatments), data analysis, methodology, manuscript writing, reviewing and editing. **RK:** Conceptualization, data generation (tumor spheroids assay, biochemistry, chemotaxis assay, animal models of tumor seeding and initiation, flow cytometry and cell sorting), data analysis, manuscript editing. **CQ:** Conceptualization, data generation (tumor spheroids assay, flow cytometry and cell sorting, animal models of tumor seeding). **JZ**: Data generation (biochemistry, flow cytometry and cell sorting), data analysis (human samples), manuscript editing. **MM:** Data generation (immunohistochemistry). **DI:** Data generation (Flow cytometry and sorting), data analysis (human samples), methodology, manuscript editing. **MC**: Data generation (immunohistochemistry, biochemistry). **CMM:** Data analysis (RNA sequencing) and data curation. **GK:** Data generation and analysis (RNA sequencing), data curation, manuscript reviewing and editing. **OM:** Conceptualization, resources, formal analysis, funding acquisition. **AF:** Conceptualization, investigation, supervision, resources, funding acquisition, data analysis, formal analysis, methodology, writing original draft, manuscript reviewing and editing.

CONFLICT OF INTEREST

The authors declare no competing interests.

ADDITIONAL INFORMATION

Supplementary information The online version contains supplementary material available at https://doi.org/10.1038/s41388-021-02174-w.

Correspondence and requests for materials should be addressed to Alessandro Fatatis.

Reprints and permission information is available at http://www.nature.com/reprints

Publisher's note Springer Nature remains neutral with regard to jurisdictional claims in published maps and institutional affiliations.